

Triggering and Guiding Electrical Discharge, and
Plasma Formation by Superposition of Laser Beams

· A Fundamental Study on the Controlled Inducing of Lightning ·

Masafumi JINNO

1997

Dedicated to my ancestors:

In the eternal flow of time,

one's life in this world is ephemeral.

Once born, nothing can escape from vanishment.

from "Atsumori" by Zeami

Preface

When I entered Kyoto University, I never thought that I would engage in the study of electrical discharge and that I would continue to research on it. At that time, I thought that an electrical discharge had no unknowns because it is a very old theme and has many predecessors. But now, I realize that this was my misunderstanding. There are many unknowns about electrical discharge and it is still now an interesting subject of research, because electrical discharge engineering is none other than the plasma engineering which is generally regarded as a frontier science. So, it was good fortune for me to engage in the research of Laser Triggering of Lightning and to be interested in electrical discharge and plasma physics.

There are many tales, which are concerned with lightning in Kyoto where I was born and grew up. A tradition of Michizane Sugawara, my ancient ancestor, is one of them. The tradition says that he took revenge upon his enemies with lightning strikes. So, I think it is Karma that I engaged in the study of laser triggering of lightning here, in Kyoto. So, now I realize that engaging in research about electrical discharge and devoting my life to research is my destiny.

Finally, I thank My ancestors.

Kyoto, my hometown

Early Spring 1997

Masafumi Jinno

Acknowledgements

I would like to express my sincere gratitude to all the people that aided me to complete this work.

First, I would like to thank Ryohei Itatani, professor emeritus of Kyoto University. I was greatly moved by his infinite eagerness for science, technology and education. He is my father of science.

I would like to express my sincere thanks to Professor Kunihide TACHIBANA of Kyoto University for his advice, encouragement and for giving me the opportunity to finish these experiments in his laboratory. I would like to express my sincere gratitude to Professor Shigeo FUJITA of Kyoto University for his continuous advice and encouragement. I would like to thank Professor Tadasu TAKUMA of Kyoto University for his guidance, valuable comments and continuous advice from my student days.

I would like to express greatly thanks to Mr. Makoto KUBO, Instructor of Kyoto University, for his encouragement, advice and teaching me various techniques for experiments. I would like to thank Dr. Osamu YAMAMOTO, Instructor of Kyoto University, for many discussions about the mechanism of an electrical discharge and for teaching me high voltage techniques. I would like to express gratitude to Associate Professor Yasuyoshi YASAKA of Kyoto University for discussion about Microwave Circuits and Plasma Formation, and for his encouragement.

I would like to express greatly thanks to my collaborators at Kyoto University, Messers Kazutaka OKAYAMA, Akihiro TAKETANI, Hitoshi MORIOKA, Hidetaka OZAKI, Gen NAGANO,

Hisashi NAGATA, Takashi TAKATORI and Taketo KISHI, for their great contributions to this work and their continuous encouragement. The memories of staying over night with them carrying out experiments are my precious treasures. I thank Dr. Hiromasa TAKENO, Dr. Akimitsu HATTA, Dr. Osamu SAKAI and Mr. Ichiro TAKAHASHI for their useful advice and their encouragement. Especially I would like to note that Dr. TAKENO offered the style file of \LaTeX for this theses. I also express thanks to Mr. Motonori IKEDA for his contribution to the experiments using his VTR system.

I would like to express greatly thanks to Associate Professor Masaharu AONO, Lecturer Hiroshi SAKATA and Mr. Hisayoshi KUROKAWA of Ehime University for their continuous encouragement. Especially to Dr. Masaharu AONO, I thank for his useful advice on plasma physics and an electrical discharge and for great encouragement.

I acknowledge the people who spent the hard and purposeful days at Itatani laboratory, especially Messers Toshio NOMURA, Masaki Shiina, Taku SUMITOMO, Koji Murayama, Satoshi Fukushima, Yoshihiro Ushigusa for their encouragement. I also thank my best friends Mr. Makoto YOSHIMURA, Mr. Tomoya NISHIKAWA and the all members of SURFACER, for their mental support and continuous encouragement.

I also thank Professor Robin Devonshire of Sheffield University for his encouragement at every visit to JAPAN.

This work was supported in part by Kansai Electric Co. Ltd. and by a Grant-in-Aid for Scientific Research from the Ministry of Education, and was performed during the period when the author was supported by a Fellowship of the Japan Society for the Promotion of Science for Japanese Junior Scientists.

Finally, I thank my family for their continuous support for my life devoted to research and I would like to dedicate this thesis to them and my ancestors.

TABLE OF CONTENTS

Preface	i
Acknowledgements	ii
1 Introduction	1
1.1 Laser Triggering of Lightning	1
1.2 Optical Air and Gas Breakdown	8
1.3 Laser Triggered Discharge	11
1.4 Composition of This Thesis	13
References	14
2 Plasma Formation by Superposition of Laser Beams	25
2.1 Introduction	25
2.2 Addition Law of Energy on Superposition of Two Laser Beams of the Same Wavelength	26
2.2.1 Experimental Setup	27
2.2.2 Experimental Results	27
2.2.3 Angled Superposition	27
2.3 Plasma Formation by Superposing Laser Beams	37
2.3.1 Experimental Setup	37

2.3.2	Experimental Results	41
2.3.3	Discussion	48
2.4	Summary	51
	References	52
3	Plasma Formation by Superposition of a Laser Beam and a Microwave	56
3.1	Introduction	56
3.2	Experimental Setup	57
3.3	Experimental Results	61
3.3.1	Plasma Formation by Microwave	61
3.3.2	Plasma Formation by XeCl laser	61
3.3.3	Plasma Formation by the Superposition of Microwave and XeCl laser . .	65
3.4	Discussion	69
3.5	Summary	76
	References	77
4	Triggering an Electrical Discharge by a Laser Produced Plasma	82
4.1	Introduction	82
4.2	The Correlation between an Electrical Discharge Current and a Path of Electrical Discharge Triggered by a Laser Produced Plasma	83
4.2.1	Experimental Setup	83
4.2.2	Experimental Results and Discussion	85
4.3	The Effect of Oxygen on the Delay Time of Flashover Triggered by a Laser-Produced Plasma	89
4.3.1	Experimental Setup	89
4.3.2	Experimental Results	91

4.3.3	Discussion	95
4.4	Summary	100
	References	101
5	Triggering Electrical Discharge and Guiding its Path by Weakly Ionized Channel with Different Wavelength of Laser Beams	105
5.1	Introduction	105
5.2	Experimental Equipment	109
5.3	Triggering and Guiding an Electrical Discharge with XeCl Laser	112
5.3.1	Experimental Setup	112
5.3.2	Experimental Results	114
5.3.3	Discussion	120
5.4	Triggering and Guiding an Electrical Discharge with CO ₂ Laser	124
5.4.1	Experimental Setup	124
5.4.2	Experimental Results and Discussion	125
5.5	Triggering and Guiding an Electrical Discharge with XeCl laser and CO ₂ Laser	127
5.5.1	Experimental Setup	127
5.5.2	Experimental Results	127
5.5.3	Discussion	130
5.6	Summary	133
	References	133
6	Conclusion	138

List of Figures

1.1	Schematic of the rocket triggering of lightning.	3
1.2	Schematic of the laser triggering of lightning.	4
1.3	Schematic of the Cross-Beam Laser Triggering of Lightning.	7
1.4	Schematic of the laser triggering of lightning in a cloud.	9
2.1	The experimental arrangement for verifying the energy addition law.	28
2.2	The optical breakdown probability versus laser energy.	29
2.3	Geometry of a laser beam and axes for numerical calculations.	31
2.4	Optical air breakdown probability vs distance between focal points of CO ₂ laser beams.	34
2.5	The result of numerical calculation of air breakdown probability versus laser incident angle θ	35
2.6	The result of numerical calculation of required energy for plasma formation versus laser incident angle θ in the real scale Laser Triggering of Lightning.	36
2.7	The experimental arrangement for superposing two CO ₂ laser beams.	38
2.8	The experimental arrangement for superposing two XeCl laser beams.	39
2.9	The experimental arrangement for superposing a XeCl laser beam and a CO ₂ laser beam.	40
2.10	Optical air breakdown probability p_5 superposing two CO ₂ laser beams mapped on a normalized energy plane.	42

2.11	Optical air breakdown probability p_S superposing two XeCl laser beams mapped on a normalized energy plane.	43
2.12	The optical air breakdown probability p_S versus oscillation time lag τ between two XeCl lasers.	45
2.13	The optical air breakdown probability p_S superposing a CO ₂ laser beam and a XeCl laser beam is mapped on the energy plane.	46
2.14	Photographs of an optical air breakdown plasma made by superposing a XeCl laser beam and a CO ₂ laser beam.	47
2.15	The numbers of successes and failures in producing an optical air breakdown by superposing a CO ₂ laser beam and a XeCl laser beam versus the delay time of laser oscillation from XeCl laser to CO ₂ laser τ	49
2.16	The optical wave shape of a CO ₂ laser and a XeCl laser.	50
3.1	Schematic diagram of a microwave circuit.	58
3.2	Experimental setup for superposition of a microwave and a XeCl laser beam. . .	62
3.3	A Photograph and a sketch of a plasma formed by a XeCl laser.	63
3.4	Air breakdown probability vs XeCl laser energy.	64
3.5	VTR photographs of plasma formation by superposition of a microwave and a XeCl laser.	66
3.6	Waveforms of reflected microwave power.	67
3.7	Delay time of microwave absorption vs microwave power.	68
3.8	Air breakdown probability vs microwave power.	70
3.9	Condition of XeCl laser energy and microwave power for plasma formation. . . .	71
3.10	Microwave equivalent circuit.	72
4.1	Experimental setup for observing the discharge path and the discharge current. .	84

4.2	Discharge current triggered by a XeCl laser-produced plasma.	86
4.3	Discharge triggered by a laser plasma.	87
4.4	Experimental setup for observation of the jump of delay time of discharge.	90
4.5	Delay time of discharge versus applied voltage and partial pressure of oxygen.	92
4.6	The relation between delay time of discharge and applied voltage.	93
4.7	The delay time of discharge and applied voltage in oxygen and in nitrogen.	94
4.8	Photodetachment cross sections of O_2^- and O^-	96
4.9	Collision electron detachment cross sections of O^- and O_2^-	98
4.10	Probability of attachment for electrons in oxygen.	99
5.1	Photographs of triggered and guided discharge by laser beam and laser-produced plasma.	107
5.2	Sketches of Fig.5.1	108
5.3	Arrangement of electrodes and laser beam.	111
5.4	Setup for measurement of the density of a plasma.	113
5.5	Relation between θ and V_{50}	116
5.6	Guided length of discharge path L_k and delay time of discharge τ_d versus laser incident angle θ	117
5.7	Guided length of discharge path L_k versus laser incident angle θ	118
5.8	Guided length L_k and delay time of discharge τ_d versus applied voltage V_k	119
5.9	Detected charge on the laser light path.	121
5.10	Guided length of discharge path L_g and delay time of discharge τ_d versus applied voltage V_g using XeCl laser and CO_2 laser.	129
5.11	Hybrid-Cross-Beam Laser Triggering of Lightning.	132

List of Tables

1.1	Research of triggered discharge in a long gap	6
3.1	Characteristics of the XeCl excimer laser.	60
5.1	The Characteristics of lasers used in the experiment	110
5.2	Variation of V_{50} by laser wavelength (plasma position is near the anode).	126

Chapter 1

Introduction

1.1 Laser Triggering of Lightning

All of the life on the earth receives the blessings of nature. Sometimes nature rages against the life. Lightning is one of the hard blows of nature because it strikes on the ground with huge energy and sometimes burns up fields and mountains. Lightning had been wrapped in mystery in old days for human beings and had been dreaded and venerated by them from time immemorial. This becomes clear with the fact that the god of thunder that is armed itself with lightning is described as the top of gods and goddesses in every myth in the world.

And now, in the information-oriented society much electronic equipment is used, especially computers play an important role in society. However computers are weak in an electric failure even for a moment, so a tremendous loss is caused by lightning which interrupts a stable power supply. Now, in Japan, more than half of the troubles in power lines are caused by lightning. So, the establishment of lightning protection is a social demand.

After the famous experiment of triggering lightning by B. Franklin using a kite in 1752, the studies on lightning as an electrical phenomenon have been carried out from various viewpoints. In recent years, studies on the triggering of lightning, which has its origin in B. Franklin's experiment, are carried out for the observation of lightning and for the lightning protection.

Mainly two methods have been studied as the method of triggering of lightning. One is the rocket triggering of lightning and the other one is the laser triggering of lightning.

In the rocket triggering of lightning, as shown in Fig. 1.1, lightning is triggered by the wired rocket which is connected to the ground. The rocket triggering of lightning was done first on the sea in 1965 at Florida, U.S.A by M.M.Newman et al¹⁾. In France, from 1973, many experiments of the rocket triggering of lightning have been carried out by R.P.Fieux et al.²⁾ using a rocket for hailstone protection and the wire for controlling a wired missile. They made clear the condition for triggering, and measured the lightning discharge current and the electromagnetic field. On the other hand, in Japan from 1977 triggered lightning by rocket has been observed about 200 times by K.Horii et al³⁾. They got the data of the lightning discharge and of the structure of thundercloud. Essentially, the rocket triggering of lightning was developed for lightning observation, and never for lightning protection. So it is difficult to apply this method on lightning protection because of some risks such as: the falling of a miss-fired rocket with steal wire and the necessity of a large area for handling explosives. Since most electrical power lines are in the mountains in Japan, this method is not suitable for lightning protection.

In addition, there is a derivation from rocket triggering of lightning, the water triggering of lightning. In this method, a column of water made by compressed air substitutes for rocket and steal wire. This method inherits the weak points of rocket triggering of lightning such as lacking of immediate action and of high repetition.

Another method, the laser triggering of lightning, is good in high repetition and immediate action. This method has its origin in the Laser Lightning Rod System (LLRS) proposed by Ball in 1974⁴⁾. As shown in Fig. 1.2, lightning is triggered and guided by a plasma channel made by a laser beam. Ball mentioned some advantages of LLRS such as movability of the system and easy tuning of timing of laser oscillation. The experiments on the model of LLRS were carried out by Aleksandrov et al⁵⁾. They reported that the plasma channel of 1m length works

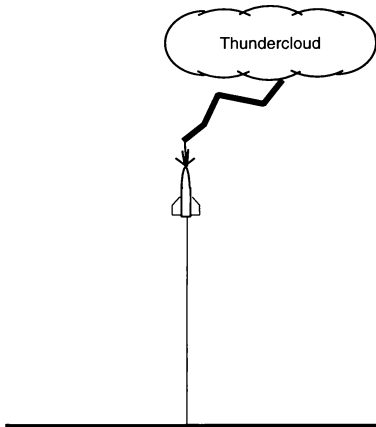


Fig. 1.1: Schematic of the rocket triggering of lightning.

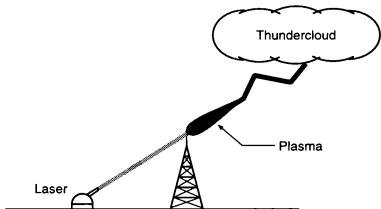


Fig. 1.2: Schematic of the laser triggering of lightning.

equal to the electrode of 4.8m height when the plasma is produced on the top of an electrode of 3.8m height. The actual laser triggering of lightning was tried in 1979 in U.S.A. At that time, though a plasma channel formation at a height of 1.5km succeeded, lightning was never triggered.

In Japan, the study of laser triggering of lightning was started in the early 1980's^{6,7)}. In recent years there has been a growing interest in laser triggering of lightning due to the development of high power lasers. Many researchers started the study and they proposed two methods. One uses a laser-produced plasma channel made by one high power laser⁸⁻¹⁷⁾. The other uses a weakly ionized channel made by a UV laser^{18,19)}. In addition, the method which produces a plasma by laser irradiation to a thundercloud directly is proposed²⁰⁾. Moreover Kawasaki et al.²¹⁾ have been trying the field experiment of laser triggering of lightning. However they have never achieved triggering of actual lightning. The study on laser triggering of lightning has also started in Korea²²⁾. The researchers and the gap length are shown in Table 1.1. The maximum length of triggered gap by the former method is 16m with 300J of laser beam¹⁴⁾. In order to trigger a discharge in the several tens or 100m-class gap, an extra-high power laser seems to be required.

Due to the problem of self-absorption and reflection of laser energy by the plasma itself, it is difficult to produce a long plasma channel by only one beam. In order to solve this problem an extremely high power laser is required. Then as the way to reduce required power, the beam dividing method and the multi focus method are proposed⁴⁷⁾. However, even both of them still seem to require a high power laser. This is the weak point of single beam laser triggering of lightning.

As the resolution for this weak point of the single beam method, the author's group proposed the Cross-Beam Method as shown in Fig. 1.3. In this method, two or more laser beams are used, and plasmas are formed by the superposition of them. The energy of each laser beam is below

Table 1.1: Research of triggered discharge in a long gap

Research Group	laser	Voltage	Gap length	references
Koopman et al.	Nd:glass (77J)	I.G. +350kV	0.71m	23-25
Naval Res. Lab.	CO ₂ (1kJ)	I.G. +360kV	2m	26-28
	Nd:glass (60J)	I.G. +250kV	1m	27, 29-33
M.I.Kalinin Poltech. Inst.	Nd:glass (100J)	I.G. +2.7MV	6m	5, 34
Ivanov et al.	Nd:glass (150J)	I.G. -1.947MV	2.67m	35
Asinovskii et al.	Nd:glass (70J)	I.G. -0.6MV	0.4m	36-38
Keio Univ.	CO ₂ (45J)	I.G. -320kV	1.75m	39
	CO ₂ (45J)	I.G. -1.44MV	3m	40, 41
Osaka Univ. etc.	CO ₂ (100J)	I.G. -1.0MV	8.5m	42-44
Kyusyu Univ etc.	CO ₂ (45J)	I.G. -1.0MV	1.25m	11, 45
	CO ₂ (300J)	I.G. -3.0MV	16m	14
C'RIEPI	CO ₂ (45J)	I.G. -3.2MV	7m	10
	CO ₂ (150J)	I.G. -3.3MV	13m	46

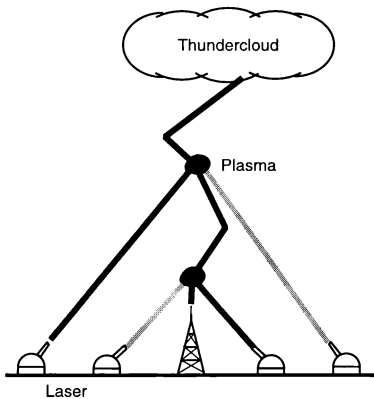


Fig. 1.3: Schematic of the Cross-Beam Laser Triggering of Lightning.

the threshold energy of plasma formation. The plasmas, which are produced by superposition of laser beams, are disposed in a line. Consequently they trigger and guide the lightning. Since different wavelengths of laser beams and moreover microwaves can be used in this method, the effective plasma formation is expected. Since a plasma can be formed anywhere by this method, not only ground stroke discharge but also inter-clouds discharge may be triggered. Moreover this method is expected to extinguish electric charges by a plasma formed in a thundercloud as shown in Fig. 1.4. This Cross-Beam method will reduce the required power of each beam for plasma formation. This is a great advantage because it is difficult to develop a high power laser at low cost.

For practical use, the Cross-Beam method has two key-problems. One is to prove the plasma formation by superposition of laser beams each of which has energy below the threshold of plasma formation. The other is to prove triggering a discharge and guiding its path by laser-produced plasmas. In this study these two key-subjects are solved.

Before the description of this study, the previous studies on plasma formation by a laser beam and on the laser triggered discharge are reviewed.

1.2 Optical Air and Gas Breakdown

When a laser beam is focused in the air and when the intensity of a laser field becomes over 10^6 – 10^7 V/cm, an optical breakdown is produced with a flash and a sharp crack and consequently a plasma is formed. This phenomenon was reported first by Maker in 1962⁴⁸⁾. After that there have been many studies of optical breakdown in air and gases.

Haught⁴⁹⁾ reported that in rare gases (Ne, He, Ar) the breakdown threshold of intensity of a ruby laser ($\lambda = 694.3\text{nm}$) is higher than that of a glass laser ($\lambda = 1060\text{nm}$) though the photon energy of a ruby laser is higher than that of a glass laser. Similar results in helium, in oxygen and in nitrogen were reported by Tomlinson⁵⁰⁾. The breakdown threshold of intensity versus laser

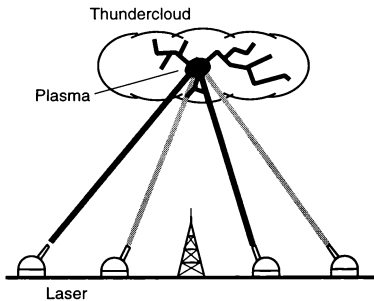


Fig. 1.4: Schematic of the laser triggering of lightning in a cloud.

wavelength were measured by Buscher et al.⁵⁴¹, and they reported that at a certain wavelength the breakdown threshold has minimum value. Similar characteristics were reported in air by Barthelemy⁵⁴², in xenon and in argon by Alcock⁵⁴³. Raizer et al.⁵⁴⁴ arranged the breakdown threshold in air by ruby laser⁵⁴⁵, glass laser⁵⁴⁶, HF laser⁵⁴⁶, DF laser⁵⁴⁶, CO₂ laser⁵⁴⁷, and D₂O laser⁵⁴⁸. Their experimental results show that the breakdown threshold becomes higher as the wavelength becomes shorter in the range of wavelength from visible to infrared.

The breakdown threshold of ruby laser versus gas pressure was reported by Minck et al.⁵⁴⁹, Haught et al.⁴⁹⁹, and Gill et al.⁶⁰⁰ They reported that the threshold decreases first with the reduction of the gas pressure and that it increases after being the minimum value.

Litvak et al.⁶¹¹ reported the time decay of electron temperature and density of a laser-produced plasma in hydrogen. In 1 μ sec from the start of plasma formation, the density changes from 10^{19}cm^{-3} to 10^{17}cm^{-3} , and temperature changes from 10^5K to 10^4K . Alcock et al.⁶²¹ also reported the time decay of the electron density of an air breakdown plasma produced by ruby laser.

When a high power laser beam is focused by a lens or a concave mirror of long focal length, a plasma channel of more than 10m length can be formed. However, the plasma channel is not a continuous one, it consists of many beads like plasmas formed near the focal point. Parfenov et al.⁶³⁰ reported that they succeeded in 50m length of plasma formation by 5GW glass laser. Uchiyama et al.³⁹⁹ succeeded in 30m length of plasma formation by 50J CO₂ laser, and at that time they measured that the plasma transmits 40% of injected laser energy. Then they calculated the required energy of CO₂ laser for 100m length of plasma formation as 150J referring to their experimental results. Yoshida et al.^{64, 65} reported the effect of UV(KrF) laser preionization on a breakdown by a CO₂ laser in helium. However, there has been no study on the power relation between laser beams when a plasma is formed by superposing two laser beams.

The mechanism of optical breakdown is accounted for by two theories. One is the "multi-photon ionization" ⁶⁶⁻⁶⁹⁾, and the other is the "inverse bremsstrahlung process" ⁷⁰⁻⁷⁸⁾. The "microwave breakdown theory" was shown to be a classical description of the "inverse bremsstrahlung process" ^{74,76-78)}. The latter theory agrees well with the experimental results of the breakdown threshold of laser intensity versus gas pressure. In addition, in the case of the long plasma channel formation by a CO₂ laser beam the mechanism of plasma formation seems to be thermal heating of aerosol or small particles⁷⁹⁾. However they account for the process of plasma formation by only one laser beam. Still now, there is no theory accounting for the plasma formation by superposition of laser beams.

All the experiments, except for that by Yoshida et al.^{64,65)}, have been carried out on optical breakdown by focusing only one laser beam. So, in this study, as the fundamental research for the Cross-Beam Laser Triggering of Lightning, the plasma formation by superposition of laser beams is investigated.

1.3 Laser Triggered Discharge

The studies on the laser triggered discharge in a short gap have been carried out for the Laser Triggered Spark Gap(LTSG). In the LTSG, metal vaporized plasma is produced by laser irradiation, and the plasma triggers an electrical discharge. The mechanism of LTSG was reported by Noguchi et al.⁸⁰⁾ They reported that the discharge has four styles changing with applied voltage between the gap. They also reported the relation between the minimum voltage for triggering a discharge and gap width. The delay time of discharge versus the applied voltage was observed and reported by Bettis et al.⁸¹⁾

The author's group has investigated laser triggered discharge as the fundamental research of the Cross-Beam method. They reported⁸²⁾ that a discharge path is guided by a laser beam focused between electrodes, and that the photodetachment of O⁻ is the dominant process in

the mechanism of laser triggered discharge.

In recent years, in addition to the author's group, Hidaka et al.⁸³⁾ has studied on triggering and guiding an electrical discharge by a laser-produced plasma. However, the mechanism of trigger and guide effect of a plasma produced between electrodes is still unknown.

In this study, the delay time of a discharge triggered by a laser-produced plasma versus applied voltage between electrodes in oxygen-nitrogen mixture is investigated as the fundamental research of revealing the mechanism of the laser triggered discharge.

Koopman et al.²⁵⁾ reported that Nd-glass laser irradiation before the applying impulse voltage reduces the delay time of discharge and guides a discharge path along the laser-produced plasma in a 67cm gap. They also reported²⁶⁾ that the chain like plasmas produced by a CO₂ laser have a guiding effect when the electric field is over 1kV/cm, and that the discharge propagation velocity becomes maximum when the delay time of voltage application is in the range of 10-100 μ sec. These experiments were carried out in the 50-180cm gap, and the discharge propagation is accelerated by laser irradiation and laser-produced plasmas.

In Japan, as shown in Table.1.1, many experiments of laser triggered discharge in a meter-class long gap have been carried out after the experiment by Uchiyama et al. in 1988³⁹⁾. The gap length has become longer with increased laser power and applied voltage between the gap. Now the maximum length of laser triggered gap is 16m⁴⁾. However, a 10meter-class gap seems to be the upper limit determined by the laser power and the characteristics of high voltage generator. Then some research groups have started to apply the hybrid-system proposed by the author's group⁸⁴⁾. This method is the refinement of the Cross-Beam method and it uses different laser beam wavelengths. So, in this study, the effect of using a CO₂ laser with a XeCl laser on triggering and guiding an electrical discharge is investigated.

1.4 Composition of This Thesis

This work was carried out in order to establish fundamentally the Cross-Beam Laser Triggering of Lightning. Two key-points of the Cross-Beam method are the plasma formation by superposition of laser beams and the triggering and guiding of an electrical discharge by both the ball-shaped laser-produced plasmas and the weakly ionized channel.

In Chapter 2, the plasma formation by superposition of laser beams is examined using a CO_2 laser and a XeCl laser. In this experiment, the energy of each laser beam is below the breakdown threshold. The energy addition law is established experimentally. The combinations of same and different wavelengths are examined, and plasma formation was achieved in these combinations. Then it is shown that the combination of a CO_2 laser and a XeCl laser is effective for plasma formation.

Steady-state plasma formation and heating by superposition of a microwave and a XeCl laser are examined in Chapter 3. The reduction of the breakdown threshold of the electric field intensity of the microwave is calculated using an equivalent circuit. It is shown that the superposition of a microwave and a XeCl laser is effective for plasma formation and heating, and that a steady-state plasma can be produced in the open air by superposition of them.

In Chapter 4, the correlation between the path of a triggered electrical discharge by a XeCl laser-produced plasma and the discharge current is observed. It is found that the current has the second peak between the first peak immediately after the laser injection and the flashover when the discharge path avoids the laser-produced plasma. On the other hand it is found that the current has no peak between the first peak and the flashover when the discharge path goes through the plasma. Moreover, the delay time of an electrical discharge in the gap triggered by a laser-produced plasma is investigated in the mixture of oxygen and nitrogen in Chapter 4. It is shown that the leap of delay time occurs when oxygen exists in the mixture. By calculation of the electron detachment cross-sections of O^- and O_2^- , it is shown that the leap is caused by

the changing of negative charge between electron and oxygen negative ion O^- according to the changing of applied voltage between the gap.

The experiment on triggering and guiding an electrical discharge by a weakly ionized channel produced by a XeCl laser and a CO_2 laser is carried out in Chapter 5. It is shown that a XeCl laser produces a weakly ionized channel on its light path, and that a CO_2 laser never produces it. The electron density required to guide an electrical discharge path is measured as more than $1.1 \times 10^{16} \text{cm}^{-3}$. It is shown that the combination of a laser-produced plasma and a weakly ionized channel, which are obtained by a XeCl laser and a CO_2 laser, is effective for triggering and guiding an electrical discharge. According to the experimental results, the Hybrid-Cross-Beam Laser Triggering of Lightning is proposed.

Finally, in Chapter 6, this work will be summarized as a conclusion.

References

- [1] M. M. Newman et al. : "Triggered lightning stroke at very close range", *J. Geophys. Res.*, **72**, 4761 (1967)
- [2] R. P. Fieux, C. H. Gary, B. P. Hutzler, A. R. Eybert-Berard, P. L. Hubert, A. C. Meesters, P. H. Perroud, J. H. Hamelin and J. M. Person : "Research on artificially triggered lightning in France". *IEEE Transactions on Power Apparatus and Systems*, **PAS-97**, 725-733 (1978)
- [3] K. Horii et al. : "Outline of rocket-triggered current and voltage measurement in winter 1991", *1992 National Convention Records of I.E.E.J.*, No.1275 (1992) [in Japanese]
- [4] Leonard M. Ball. : "The laser lightning rod system: Thunderstorm domestication." *Applied Optics*, **13**, 2292-2296 (1974)
- [5] G. N. Aleksandrov, V. L. Ivanov, G. D. Kadzov, V. A. Parfenov, L. N. Pakhomov, V. Yu. Petrun'kin, V. A. Podelevskii and Yu. G. Selezov. : "Effect of a laser-produced ionization channel on a long discharge in air", *Soviet Physics Technique Physics*, **22**:1233-1234 (1977)
- [6] T. Shindo and T. Suzuki : "Laser-induced gas breakdown and its application for lightning protection", *The report of CRIEPI*, No.182010 (1982)

- [7] A. Sumita, T. Narahara, M. Kubo and R. Itatani : "The effect of laser irradiation on the characteristics of flashover", *1982 Convention Records of I.E.E.J. in Kansai*, G1-14 (1982) [in Japanese]
- [8] T. Shindo, Y. Aihara, M. Miki and T. Suzuki : "Model Experiments of Laser Triggered Lightning", *IEE Transactions on Power Delivery*, **8**, 311-317 (1993)
- [9] T. Shindo, M. Miki, J. Wada and Y. Aihara : "Simulation of Plasma Production with Laser Propagation", *Trans. I.E.E.J.*, **115-A**, 589-594 (1995) [in Japanese]
- [10] M. Miki, A. Wada, T. Shindo and Y. Aihara : "Positive Discharge Guided by CO₂ Laser Radiation in Air", *Trans. I.E.E.J.*, **115-A**, 644-651 (1995) [in Japanese]
- [11] C. Honda, T. Takuma, K. Muraoka, M. Akazaki, F. Kinoshita and O. Katahira : "Characteristics of Discharge Induced by Laser-Generated Plasmas", *Trans. I.E.E.J.*, **113-B**, 994-1002 (1993) [in Japanese]
- [12] T. Ikegami, T. Kakiuchi, K. Ebihara and M. Akazaki : "Characteristics of Electrical Discharge Induced by Excimer Laser", *Trans. I.E.E.J.*, **114-A**, 31-39 (1994) [in Japanese]
- [13] T. Tsuji, C. Honda, M. Uchiumi, T. Tanaka, K. Muraoka, T. Takuma, M. Akazaki, F. Kinoshita and O. Katahira : "Characteristics of Laser-Produced Plasma in Atmospheric Air", *Trans. I.E.E.J.*, **115-A**, 583-588 (1995) [in Japanese]
- [14] M. Uchiumi, H. Irino, T. Makino, T. Tanaka, K. Muraoka, G. Baitsur, F. Kinoshita, O. Katahira, C. Honda, T. Tsuji and M. Akazaki : "Production of an Effective Laser Air-Breakdown Channel in inducing a Long-Gap Discharge and Its Elongation", *Trans. I.E.E.J.*, **115-A**, 614-621 (1995) [in Japanese]

- [15] S. Ihara, T. Maiguma, S. Satoh, M. Ishimine and C. Yamabe : "Characteristics of a Plasma Production and a Laser-Induced Discharge by a CO₂ Laser on DC electric field", *Trans. I.E.E.J.*, **115-A**, 630-636 (1995) [in Japanese]
- [16] T. Uchiyama : "Laser Triggering Lightning". *Jpn. J. Plasma and Fusion*, **70**, 168-172 (1994) [in Japanese]
- [17] D. Wang, Z.-I. Kawasaki, K. Matsuura, Y. Shimada, S. Uchida, C. Yamanaka, E. Fujiwara, Y. Izawa, N. Simokura and Y. Sonoi : "A preliminary study on laser-triggered lightning", *Journal of Geophysical Research*, **99**, 16907-16912 (1994)
- [18] K. Nakamura, T. Suzuki, C. Yamabe and K. Horii : "Fundamental Research for Lightning Trigger Experiment by Using UV Lasers", *Trans. I.E.E.J.*, **113-B**, 1265-1273 (1993) [in Japanese]
- [19] M. Miki, A. Wada and T. Shindo : "Artificial triggered lightning using ultraviolet laser-guiding of the electrical discharges by an excimer laser" *Rev. Laser Eng.*, **24**, 564-571 (1996) [in Japanese]
- [20] H. Takeno, M. Cho, X. Wang and K. Arai : "Fundamental study on laser induced discharge in cloud due to optical and electrical measurements with numerical simulations", *Proceedings of 9th International Symposium on High Voltage Engineering*, Vol.6, 6771-6774 (1995)
- [21] S. Uchida, Y. Shimada, H. Yasuda, K. Tsubakimoto, S. Motokoshi, C. Yamanaka, T. Yamanaka, H. Fujita, K. Matsuura, Z. Kawasaki, T. Ushio, T. Watanabe, W. Daohong, M. Adachi and Y. Ishikubo : "The field experiments of laser triggered lightning", *Rev. Laser Eng.*, **24**, 547-555 (1996) [in Japanese]

- [22] Yong-Moo Chang and Hyung-Boo Chang : "Basic study on laser triggered lightning - the generation of plasma channel by CO₂ laser". *Trans. Korean Inst. Electr. Eng.*, **45**, 289-293 (1996)
- [23] J. R. Vaill et al. : "Propagation of high-voltages streamers along laser-induced ionization trails". *Appl. Phys. Lett.*, **17**, 20 (1970)
- [24] David W. Koopman et al. : "Channeling of an ionizing electrical streamer by a laser beam", *J. Appl. Phys. Lett.*, **42**, 1883 (1971)
- [25] David W. Koopman and K. A. Saum : "Formation and guiding of high-velocity electrical streamers by laser-induced ionization", *J. Appl. Phys.*, **44**, 5328-5336 (1973)
- [26] J. R. Greig, D. W. Koopman, R. F. Fernsler, R. E. Pechacek, I. M. Vitkovitsky, and A. W. Ali : "Electrical discharges guided by pulsed CO₂-laser radiation" *Physical Review Letters*, **41**, 174-177 (1978)
- [27] J. R. Greig et al : "Channel cooling by turbulent convective mixing". *Phy. Fluids*, **28**, 2357 (1985)
- [28] K. R. Stalder et al : "Electrical conductivity measurements of laser-guided and exploding wire discharges in air". *SRI Report*, **88**, 292 (1989)
- [29] R. Fernsler et al : "Interaction of laser-induced ionization with electric fields", *Proc. AIAA 13th Fluid & Plasma Dynamics Conference*, AIAA-80-1380 (1980)
- [30] D. P. Murphy et al. : "Electron beam transport the atmospheric in reduced-density, current carrying channels". *Pre. 9th Int. Symp. on Engineering Prob. in Fusion Research*, **1**, 15-18 (1981)

- [31] J. R. Greig et al. : "Laser-guided electric discharge in atmosphere", *Proc. 7th. Int. Conf. on Gas Discharges and Their Applications*, pp. 464 (1982)
- [32] Timothy. J. Dwyer et al. : "On the feasibility of using an atmospheric discharge plasma as an RF antenna", *IEEE Transaction on antenna and propagation*, **AP-32**, 141 (1984)
- [33] J. D. Colvin : "An empirical study of the nuclear explosion-induced lightning seen on IVY-MIKE", *J. Geophys. Res.*, **92**, 5696 (1987)
- [34] G. N. Aleksandrov et al. : "Orientation of an electric discharge along a long laser spark", *Sov. Tech. Phys. Lett.*, **15**, 628 (1989)
- [35] O. G. Ivanov, et al. : "Effect of a laser spark on the discharge characteristics of a long air-filled gap", *Tech. Phys.*, **39**, 645 (1994)
- [36] E. I. Asinovskii et al. : "pulsed electric discharge in atmospheric-pressure air guided by a long laser spark", *Sov. Tech. Phys. Lett.*, **13**, 102 (1987)
- [37] E. I. Asinovskii et al. : "Ability of a laser spark to guide an electric discharge", *Sov. Tech. Phys. Lett.*, **14**, 18 (1988)
- [38] A. Abramov et al. : "Guided discharges generator with 3MV voltage and 1013V/s steepness", *Preprint IVTAN*, **No.5-348** (1992)
- [39] T. Uchiyama, M. Hirohashi, H. Miyata and T. Sakai : "Study of Triggering Lightning by using TEA CO₂ Laser", *Rev. Laser Eng.*, **16**, 267-277 (1988) [in Japanese]
- [40] M. Hirohashi et al. : "Triggered Lightning by Laser", *1989 National Convention Records of I.E.E.J.*, **S.2-17** (1989) [in Japanese]
- [41] M. Hirohashi et al. : "Laser Triggering of Lightning", *Journal of The Japan Research Group of Electrical Discharges*, **No.123**, 45 (1989) [in Japanese]

- [42] E. Fujiwara, Y. Izawa, Z. Kawasaki, K. Matura and C. Yamanaka : "Laser Triggered Lightning", *Rev. Laser Eng.*, **19**, 22-31 (1991) [in Japanese]
- [43] M. Nishimura, Y. Kono, Z. Kawasaki, K. Matura, E. Fujiwara, C. Yamanaka, K. Nakamura, T. Nagai, Y. Sonoji and S. Nakatani : "Fundamental experiments on Laser Triggered Lightning by CO₂ Laser (III)", *I.E.E.J. Papers of HV and ED*, **HV-91-73**, **ED-91-156** (1991) [in Japanese]
- [44] T. Nagai, Y. Sonoji, E. Fujiwara, Y. Izawa, Z. Kawasaki, K. Matura and C. Yamanaka : "Fundamental experiments on Laser Triggered Lightning by CO₂ Laser (V)", *I.E.E.J. Papers of HV and ED*, **HV-92-14**, **ED-92-76** (1992) [in Japanese]
- [45] C. Honda, T. Takuma, K. Muraoka and M. Akazaki : "Laser triggered discharge and measurements of it", *Journal of The Japan Research Group of Electrical Discharges*, **No.138**, 17-25 (1992) [in Japanese]
- [46] M. Miki et al. : *The report of CRIEPI*, T94076 (1995) [in Japanese]
- [47] T. Shindo and S. Sasaki : "The Developing of Lightning Protection by Laser and Future Problem", *Journal of I.E.E.J.*, **111**, 739-746 (1991)
- [48] P. D. Maker, R. W. Terhune and C. M. Savage : "Optical Harmonic Generation", *Quantum Electronics 2*, Columbia Univ. Press, pp. 1559-1576 (1964)
- [49] A. F. Haught, R. G. Meyerand, Jr. and D. C. Smith : "PHYSICS OF QUANTUM ELECTRONICS Conference Proceedings (Electrical Breakdown of Gases by Optical Frequency Radiation)", McGRAW-HILL BOOK COMPANY, pp. 509-519 (1966)
- [50] R. G. Tomlinson, E. K. Damon and H. T. Buscher : "PHYSICS OF QUANTUM ELECTRONICS Conference Proceedings (The Breakdown of Noble and Atmospheric Gases by

- Ruby and Neodymium Laser Pulses)", McGRAW-HILL BOOK COMPANY, pp. 520-526 (1966)
- [51] H. T. Buscher, R. G. Tomlinson and E. K. Damon : "FREQUENCY DEPENDENCE OF OPTICALLY INDUCED GAS BREAKDOWN", *Phys. Rev. Lett.*, **15**, 847-849 (1965)
- [52] C. Barthélemy, M. Leblanc and M. Boucault : "Variation du seuil de claquage de l'air en fonction de la longueur d'onde de l'irradiation laser", *COMPTES RENDUS HEBDOMADAIRES DES SÉANCES DEL'ACADÉMIE DES SCIENCES B(Paris)*, **266B**, 1234-1235 (1968)
- [53] A. J. Alcock, C. DeMicelies and M. C. Richardson : "WAVELENGTH DEPENDENCE OF LASER-INDUCED GAS BREAKDOWN USING DYE LASERS", *Appl. Phys. Lett.*, **15**, 72-73 (1969)
- [54] Yu. P. Raizer : "Optical discharges", *Sov. Phys. Usp.*, **23**, 789-806 (1980)
- [55] I. Mayer and P. Stritzke : "Shock waves and ionizing radiation in plasmas produced by a mode-locked laser", *J. Phys. D.:Appl. Phys.*, **10**, 1635-1641 (1977)
- [56] M. J. Soileau : "Air breakdown by pulsed-laser radiation in the 2.7-and 3.8- μm region", *Applied Physics Letters*, **35**, 309-311 (1979)
- [57] C. H. Chan, C. D. Moody, and W. B. McKnight : "Significant loss mechanics in gas breakdown at 10.6 μ ", *J. Appl. Phys.*, **44**, 1179-1188 (1973)
- [58] P. Woskobonikow, W. J. Mulligan, H. C. Praddaude, and D. R. Cohn : "Submillimeter-laser-induced air breakdown", *Applied Physics Letters*, **32**, 527-529 (1978)

- [59] R. W. Minck and W. G. Rado : "PHYSICS OF QUANTUM ELECTRONICS Conference Proceedings (Investigation of Optical Frequency Breakdown Phenomena)", McGRAW-HILL BOOK COMPANY, pp. 527-537 (1966)
- [60] D. H. Gill and A. A. Dougal : "BREAKDOWN MINIMA DUE TO ELECTRON-IMPACT IONIZATION IN SUPER-HIGH-PRESSURE GASES IRRADIATED BY A FOCUSED GIANT-PULSE LASER", *Phys. Rev. Lett.*, **15**, 845-847 (1965)
- [61] M. M. Litvak and David F. Eddwards : "Electron recombination laser-produced hydrogen plasma", *J. Appl. Phys.*, **37**, 4462-4474 (1966)
- [62] A. J. Alcock and S. A. Ramsden : "Two wavelength interferometry of laser-induced spark in air", *Applied Physics Letters*, **8**, 187-188 (1966)
- [63] V. A. Parfenov et al. : *Soviet Technical Physics Letters*, **2**, 286 (1976)
- [64] S. Yoshida, J. Sasaki, Y. Arai, M. P. Lei, K. Tateishi and T. Uchiyama : "Effect of UV preionization on optical breakdown induced by a pulsed CO₂ laser", *J. Appl. Phys.*, **58**, 620-622 (1985)
- [65] S. Yoshida, J. Sasaki, Y. Arai, and T. Uchiyama : "Effect of UV laser preionization on CO₂-laser-induced optical breakdown", *J. Appl. Phys.*, **58**, 4003-4005 (1985)
- [66] L. V. Keldysh : "IONIZATION IN THE FIELD OF A STRONG ELECTROMAGNETIC WAVE", *Soviet Phys. JETP*, **20**, 1307-1314 (1965)
- [67] A. Gold and H. B. Bebb : "THEORY OF MULTIPHOTON IONIZATION", *Phys. Rev. Lett.*, **14**, 60-63 (1965)
- [68] H. B. Bebb and A. Gold : "Multiphoton Ionization of Hydrogen and Rare-Gas Atoms", *Phys. Rev.*, **143**, 1-24 (1966)

- [69] B. A. Tozer : "Theory of the Ionization of Gases by Laser Beams", *Phys. Rev.*, **137**, A1665-A1667 (1965)
- [70] R. G. Meyerand, Jr. and A. F. Haught : "Gas breakdown at optical frequencies", *Physical Review Letters*, **11**, 401-403 (1963)
- [71] R. G. Meyerand, Jr. and A. F. Haught : "Optical-energy absorption and high-density plasma production", *Physical Review Letters*, **13**, 7-9 (1964)
- [72] J. K. Wright : "Theory of the electrical breakdown of gases by intense pulses of light", *Proc. Phys. Soc.*, **84**, 41-46 (1964)
- [73] P. F. Browne : "Mechanism of gas breakdown by lasers", *Proc. Phys. Soc.*, **84**, 1323-1332 (1965)
- [74] Ya. B. Zeldovich and Yu. P. Raizer : "Cascade ionization of a gas by a light pulse", *Sov. Phys. -JETP*, **20**, 772-780 (1964)
- [75] D. D. Ryutov : "Theory of breakdown of noble gases at optical frequencies", *Sov. Phys. -JETP*, **20**, 1472-1479 (1965)
- [76] K. Kawabe, Y. Yasojima and Y. Inuishi : "A Speculation on Mechanism of Ionization and Breakdown of Gases by Laser", *KAKUYUGO KENKYU*, **16**, 322-336 (1966) [in Japanese]
- [77] K. Kawabe, Y. Yasojima and Y. Inuishi : "Mechanism of Gas Breakdown by Laser Pulse", *KAKUYUGO KENKYU*, **19**, 187-198 (1967) [in Japanese]
- [78] Y. Yasojima, K. Kawabe and Y. Inuishi : "Theory on Mechanism of Ionization and Breakdown in Gases by Intense Laser Pulse", *Technol. Repts. Osaka Univ.*, **17**, 339-406 (1967)
- [79] D. E. Lencioni : "The effect of dust on 10.6 μ m laser-induced air breakdown", *Appl. Phys. Lett.*, **23**, 12-14 (1973)

- [80] T. Noguchi, M. Yano, T. Shimomura and K. Horii: *Trans. I.E.E.J.*, **92-A**, 449 (1972) [in Japanese]
- [81] J. R. Bettis and A. H. Guenthe: *IEEE Journal of Quantum Electronics.*, **QE-6**, 483 (1970)
- [82] M. Kubo, R. Itatani and S. Matsumura : "Basic Research for Laser Triggered Lightning - Influence of Wavelength of Laser on Atmospheric Spark Discharge -", *Trans. I.E.E.J.*, **112A**, 620-628 (1992) [in Japanese]
- [83] K. Hidaka, D. Sakai and T. Kouno : "Laser Trigger Effect on Induced Electrical Discharge", *Trans. I.E.E.J.*, **115-A**, 622-629 (1995) [in Japanese]
- [84] M. Jinno, M. Kubo and R. Itatani: "Triggering Discharge and Guiding Discharge Path by weak Ionized Channel with Different Wavelength Laser Beams", *Trans. I.E.E.J.*, **115-A**, 595-604 (1995) [in Japanese]

Chapter 2

Plasma Formation by Superposition of Laser Beams

2.1 Introduction

After the first report of an optical air breakdown by Maker in 1962¹⁾, there have been many studies of optical breakdown in air and gas (called simply "breakdown" or "plasma formation"). The relationship of an electric field of a laser beam required for a plasma formation versus the gas pressure²⁻⁸⁾ and versus the laser wavelength^{5,7,9-11)} was observed. All of the studies were made for the case focusing only one laser beam except for the study carried out by Yoshida et al.^{12,13)} They reported the effect of UV(KrF) laser preionization on a breakdown in helium by a CO₂ laser. However, there has been no study on the power relation of superposing two laser beams to form an air breakdown plasma.

The author's group proposed the Laser Triggering of Lightning by superposition of laser beams named as the Cross-Beam method. They reported that an electrical discharge can be triggered and guided by the weakly ionized channel and by the plasma formed by the laser beam^{14,15)}. Moreover it was shown that a plasma is formed by the superposition of a microwave and a XeCl laser beam¹⁶⁾. However, the plasma formation by superposition of laser beams and the energy addition law in the superposition are still unproved.

In this chapter, the effect of superposition of two laser beams of the same and different

wavelengths on the open air breakdown using a CO_2 laser and XeCl lasers is described. In section 2.2, the required energy to produce a plasma is measured in the case of both single and double beams in order to establish the energy addition law. Moreover it is estimated how much this law is influenced by the laser incident angle and by the distance between their focal points. In section 2.3, plasma formation by the superposition of two laser beams is tested in three cases – $\text{CO}_2\text{-CO}_2$, XeCl-XeCl, and $\text{CO}_2\text{-XeCl}$. Then it is shown that the combination of a CO_2 laser and a XeCl laser makes plasma formation much easier. This is because a XeCl laser produces seed electrons by multiphoton ionization with its high photon energy, on the other hand a CO_2 laser heats them up by its long pulse with a high field.

The purpose of the work in this chapter is an application of the plasma formation by superposing laser beams to triggering lightning and to controlling its discharge path¹⁵⁾. If the energy addition law of laser beams holds, and if a plasma is formed by superposition of laser beams each of whose energy is limited below the threshold value of an air breakdown using a single beam, multiple crossed beams consisting of small power lasers become equivalent to a single high power laser beam. This method might be useful to reduce the difficulty and the cost to develop a high power laser for the Laser Triggering of Lightning.

2.2 Addition Law of Energy on Superposition of Two Laser Beams of the Same Wavelength

The energy loss in superposing laser beams seems to be eliminated by precise adjustment of focal points, strict synchronization of laser oscillations, and zero angle incidence between the beams. This supposition is proved by following experiments. The energy loss, which is caused by the angled superposition and by the distance between focal points, is calculated and compared with the experimental results.

2.2.1 Experimental Setup

Figure 2.1 shows the setup of this experiment in which two types of apertures were used. One is used for partitioning one beam in two and the other for a mono beam. Both apertures control the laser energy passing through the lens by changing the central angle of the open sector. In this system, a CO₂ laser ($\lambda = 10.6\mu\text{m}$) and a XeCl laser ($\lambda = 308\text{nm}$) were used. The laser energy was measured by the Joule meter (J50, MOLE(TRON).

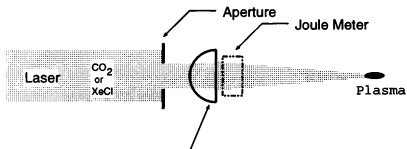
2.2.2 Experimental Results

The relation between the laser energy and the breakdown probability was observed. The result using a CO₂ laser is shown in Fig. 2.2(a), and that using a XeCl laser is shown in Fig. 2.2(b). In both figures, an open circle shows the case of not separated, and an open square shows that of separated. These results show that the relation between the breakdown probability and the laser energy. There is no difference between the case both separated and not separated. Since only one laser beam was separated into two beams, and since they were focused by the same lens simultaneously, there was no oscillation time lag and no focal deviation between the two separated beams in this system.

Thus a breakdown is produced without energy loss, when laser beams are superposed in the ideal condition, i.e. zero angle incident, the same focal point, and synchronizing laser pulse oscillations.

2.2.3 Angled Superposition

Though the addition law of energy holds in ideal condition, laser beams have incident angle, time lag, and deviation between focal points in the actual superposition. So the dependence of the air breakdown probability on the laser incident angle and on the distance between focal points of laser beams is estimated by numerical calculation model for CO₂ laser beams referring



Lens : ZnSe $f=5''$ for CO_2 Laser
 SQ $f=475\text{mm}$ for XeCl Laser

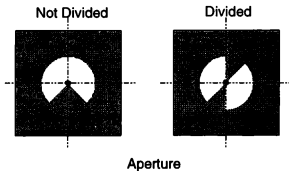


Fig. 2.1: The experimental arrangement for verifying the energy addition law. One laser beam was divided into two beams by an aperture set on the laser light path, and they were superposed in the ideal condition

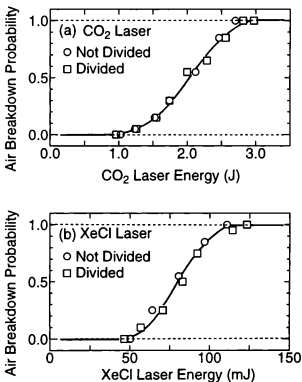


Fig. 2.2: The optical breakdown probability versus laser energy. (a) is the result using a CO₂ laser. (b) is the result using a XeCl laser. The open circle shows the result when the beam was not divided. The open square shows the result when the beam was divided. There is no difference between the results when the beam was divided and not divided.

to experimental results as follows.

Suppose that the shape of the laser beam which emerges from a lens is conical. As shown in Fig. 2.3, set the Origin at the center of the focal plane, and set the x axis along the laser light path. In this figure, r_0 is the radius of the laser beam at the focal plane, f is the focal length of the lens, and r_a is the radius of the incident laser beam into the lens.

It was shown in a previous paper¹⁵⁾ and is shown in Chapter 5 that a CO_2 laser never produces a seed electron when its energy is less than the threshold value for plasma formation. So, whenever seed electrons are produced on the focal point, they are heated and a breakdown plasma is formed as a consequence. Therefore, suppose that the breakdown probability p is in proportion to the formation probability of seed electrons, and that the formation probability of seed electrons is in proportion to the effective laser energy for plasma formation. So, the plasma formation probability is calculated as a function of the laser power density, then it is calculated as a function of laser energy, and consequently the relation between the probability and the laser incident angle is obtained as follows.

The power density $P_g(r)$ of a normalized Gaussian beam at the point A (shown in Fig. 2.3) is given by

$$P_g(r) = \frac{1}{\sqrt{2\pi}\sigma} \exp\left[-\frac{r^2}{2\sigma^2}\right], \quad (2.1)$$

where σ is a standard deviation, and r is the distance from the center of a beam to the point A, as shown in Fig. 2.3. The total power of the Gaussian beam is given as follows.

$$W_{\text{total}} = \int_0^\infty 2\pi r P_g(r) dr = \sqrt{2\pi}\sigma. \quad (2.2)$$

Since the outer part of the laser beam was cut off by an aperture in experiments, the energy through an aperture W_{in} is given by

$$W_{\text{in}} = \int_0^{r_1} 2\pi r P_g(r) dr = \sqrt{2\pi}\sigma \left(1 - \exp\left[-\frac{r_1^2}{2\sigma^2}\right]\right), \quad (2.3)$$

where r_1 is the radius of the beam on the plane vertical to the axis and containing the

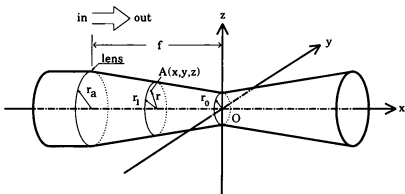


Fig. 2.3: Geometry of a laser beam and axes for numerical calculations, where f is the focal length of the lens, r_a is the radius of the beam entering the lens, r_0 is the radius of the beam at the focal plane.

point A. Then the standard deviation σ is given as follows from eqs. (2.2) and (2.3). $\sigma = r_1/\sqrt{-2\log(1-k)}$, where k is the ratio W_{in}/W_{total} .

Therefore the power density $P(r)$ at the point A is given as follows using the mean power density at the focal plane P_f .

$$P(r) = P_{\#}(r) \times \frac{\pi r_0^2 P_f}{W_{in}} = P_{\#}(r) \times \frac{\pi r_0^2 P_f}{k W_{total}} = -\frac{r_0^2 \log(1-k)}{k r_1^2} \exp\left[-\frac{r^2 \log(1-k)}{r_1^2}\right] P_f. \quad (2.4)$$

Since r_1 is given by $r_1 = |x|(r_a - r_0)/f + r_0$, and r is given by $r = \sqrt{y^2 + z^2}$, the power density $P(x, y, z)$ at the point A is given as follows.

$$P(x, y, z) = -\frac{r_0^2 \log(1-k)}{k(|x|(r_a - r_0)/f + r_0)^2} \exp\left[-\frac{(y^2 + z^2) \log(1-k)}{(|x|(r_a - r_0)/f + r_0)^2}\right] P_f. \quad (2.5)$$

Therefore the breakdown probability p is written as a function of effective power as follows.

$$p = \iiint_V G(x, y, z) dx dy dz. \quad (2.6)$$

where G is a function of power density of two laser beams $P(= P_A + P_B)$ at the point A, V is the common space formed by two crossing beams.

Suppose that the power of the laser beam, whose density is lower than the threshold value of plasma formation P_{th} , is used for production of seed electrons, and that the power, whose density is higher than P_{th} , is spent to heat up seed electrons and to lead them to a plasma. The laser power density is in proportion to the total laser power, i.e. laser energy. Therefore suppose the function G is given as follows,

$$G(x, y, z) = \begin{cases} 0, & \text{for } P < P_{th} \\ \alpha(P - P_{th}), & \text{for } P_{th} \leq P \end{cases} \quad (2.7)$$

where α is a proportional constant.

The plasma formation probability was calculated as a function of the distance between each focal point of two identical CO₂ laser beams. Each parameter was determined considering experimental results as follows, $f = 130\text{mm}$, $r_a = 15\text{mm}$, $r_0 = 0.5\text{mm}$, $P_f = 0.9P_0$, $P_{100} =$

$1.5P_0 = 1.5P_{th}$, $k=0.3$. Where P_0 is the power density when the plasma formation probability is 0. P_{100} is the density when the probability is 1.0. The calculated probability of plasma formation is shown in Fig. 2.4 as a line. In this figure, an open circle shows the results of the experiment described in the section 2.3. The calculation shows good agreement with the experimental results.

The required energy for plasma formation versus laser incident angle was calculated and is shown in Fig. 2.5. In this calculation, all parameters were the same as those above. This result shows that as the incident angle becomes larger, the energy loss becomes larger, and that at $\theta=90^\circ$, the energy loss becomes maximum and 14% excess energy is required. Since 20% excess energy was required at $\theta=90^\circ$ in the experiment as shown in Fig. 2.10, this calculation shows good agreement with the experimental results. This energy loss seems to be caused by the decrease in the common space which consists of two laser beams as the increase in the angle of intersection made by the two laser beams.

The energy loss in the real scale Laser Triggering of Lightning is simulated in the following. The distance from the earth to the bottom of a winter thundercloud is about 100m. Then each parameter was set as follows. $f=100\text{m}$, $r_A=30\text{cm}$, $r_0=3\text{cm}$, $P_I=0.9P_0$, and $P_{100}=1.5P_0=1.5P_{th}$. The required energy for plasma formation with 1.0 of probability versus laser incident angle θ is shown in Fig. 2.6. The vertical axis is normalized by the value of the energy E_{100} with which the plasma formation probability becomes 1.0 by a single laser beam. This figure gives the maximum value of the angle θ for plasma formation probability to be 1.0 when the energy of each laser beam is below the threshold value E_0 , i.e. $E_A + E_B = E < 2E_0 = 2 \times 2/3E_{100} = 1.33E_{100}$. For example, at $k = 0.7$, two laser beams should be superposed with the angle $\theta < 0.66^\circ$. In this case, the distance between the centers of the two beams at the focusing lenses is about 60cm. This geometry seems to be reasonable for real scale experiment. The upper limit of θ will become larger by using three or more laser beams.

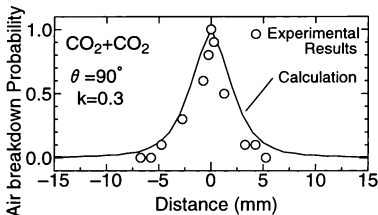


Fig. 2.4: Optical air breakdown probability vs distance between focal points of CO₂ laser beams. In this experiment (described in section 2.3), lens B was moved along its light path. The horizontal axis is the distance from the focal point of beam A to that of beam B. The open circle is the experimental result. The result of numerical calculation of the air breakdown probability is shown as a line.

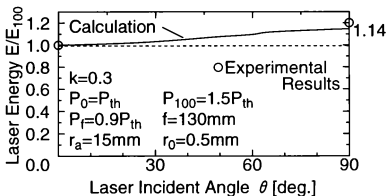


Fig. 2.5: The result of numerical calculation of air breakdown probability versus laser incident angle θ .

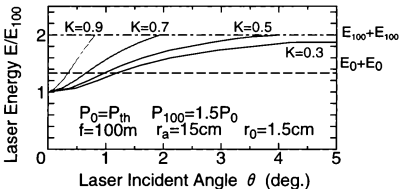


Fig. 2.6: The result of numerical calculation of required energy for plasma formation versus laser incident angle θ in the real scale Laser Triggering of Lightning.

2.3 Plasma Formation by Superposing Laser Beams

In this section, experiments of plasma formation by superposing two laser beams, i.e. CO_2 - CO_2 , XeCl - XeCl , and CO_2 - XeCl , are described. All of their energies are limited below the threshold value of making an air breakdown by a single beam. The relationship between the breakdown probability and the laser energies is observed. The effects of time difference between laser pulses and of the distance between focal points on plasma formation are measured. Moreover, the effectiveness of the combination of a CO_2 laser and a XeCl laser on plasma formation is estimated.

2.3.1 Experimental Setup

The experimental setups are shown in Fig. 2.7~2.9. One CO_2 laser ($\lambda=10.6\mu\text{m}$) and two XeCl lasers ($\lambda=308\text{nm}$) were used, and three combinations were tried. The pulse of the CO_2 laser beam has a sharp spike part of 120nsec FWHM and a long tail part of more than $2.5\mu\text{sec}$ continuing. That of the XeCl laser has only a sharp part of 30nsec FWHM. The optical pulse shape of the XeCl laser was detected by a phototube (R1193U, HAMAMATSU), and that of the CO_2 laser was detected by a photon drag detector (B749, HAMAMATSU). In the combination of two CO_2 laser beams, as shown in Fig. 2.7, one CO_2 laser beam was split into two beams and they were focused and superposed, because of the difficulty in synchronizing two different CO_2 lasers. As shown in Fig. 2.8, two XeCl laser beams were focused and superposed, since each of them was triggered by a thyatron respectively. The jitter in trigger of each laser was less than 50nsec. A CO_2 laser beam and a XeCl laser beam were superposed in the system shown in Fig. 2.9. In these three systems, focal points were adjusted referring to their burn patterns.

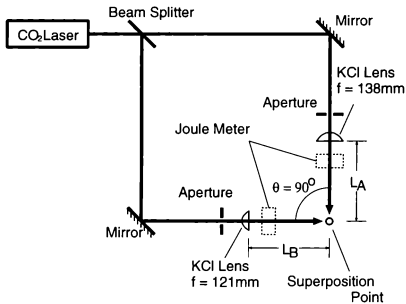


Fig. 2.7: The experimental arrangement for superposing two CO₂ laser beams. In this system, one CO₂ laser beam is split into two beams and they are focused on each other and superposed.

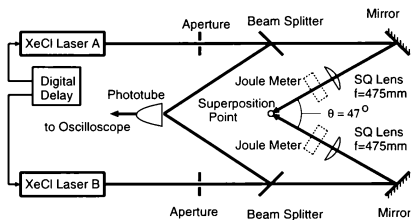


Fig. 2.8: The experimental arrangement for superposing two XeCl laser beams. In this system, two CO_2 laser oscillators are used. Two beams are focused on each other and superposed.

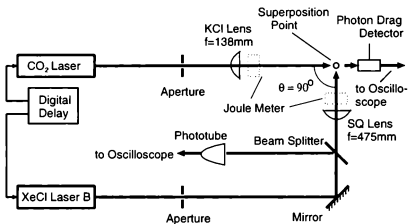


Fig. 2.9: The experimental arrangement for superposing a XeCl laser beam and a CO_2 laser beam.

2.3.2 Experimental Results

In Fig. 2.10, air breakdown probability p_S is mapped as an open circle on a normalized energy plane when two CO_2 laser beams are superposed. The open triangle shows p_A , and the open diamond shows p_B , where p_A and p_B mean the probability of each one beam injected respectively. The area A means that a plasma formation without failure is enabled by superposition of two CO_2 laser beams; the energy of both of them are limited below the threshold value of an air breakdown produced by one beam. If the addition law of energy holds, the boundary line keeping $p_A = 1.0$ agrees with the line A_1B_1 . However, the boundary swells upward. So, the segment area B bounded by this swelling boundary curve and the line A_1B_1 means an energy loss. The line A_2B_2 which tangents this segment is the sufficient condition for producing a breakdown without failure, i.e. $E_A/E_{A100} + E_B/E_{B100} > 1.20$. This means that the maximum loss is 20%, and this loss seems to correspond to angled superposition because the calculated loss is 14% as shown in Fig. 2.5 .

Figure 2.4 shows the air breakdown probability p_S versus the distance between focal points of CO_2 laser beams when they were superposed at $\theta = 90^\circ$ and the energies of both of them were kept at 90% of the critical value below which no breakdown takes place. This result shows that the distance of a focal point from another one should be within the range of $\pm 5\text{mm}$. This corresponds to 3.8% of the focal length of the lens.

In Fig. 2.11, the probability p_S in the combination of two XeCl laser beams is mapped on a normalized energy plane. In this figure the area C shows that an optical breakdown can be produced by superposition of two XeCl laser beams whose energies are limited below the threshold value of breakdown by only one beam. The area D corresponds to loss of energy as mentioned in Fig. 2.10. The sufficient condition for an optical breakdown without failure is $E_A/E_{A100} + E_B/E_{B100} > 1.87$. These results show that the energy loss in the superposition of XeCl laser beams is larger than that of CO_2 laser beams. This excess energy loss at superposi-

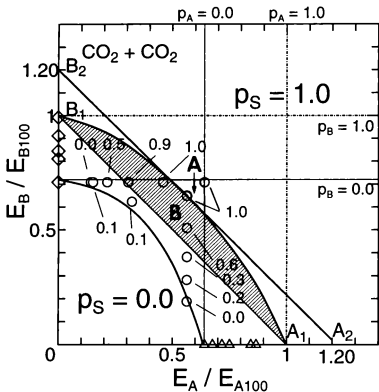


Fig. 2.10: Optical air breakdown probability p_s superposing CO_2 laser beams is mapped on a normalized energy plane. Each axis is normalized by the value of the threshold energy when each beam's air breakdown probability p_A or p_B becomes 1.0 (100%). The area A shows that an optical air breakdown can be produced without failure by superposing two CO_2 laser beams which can not produce an optical air breakdown by only one beam. The area B shows the energy loss.

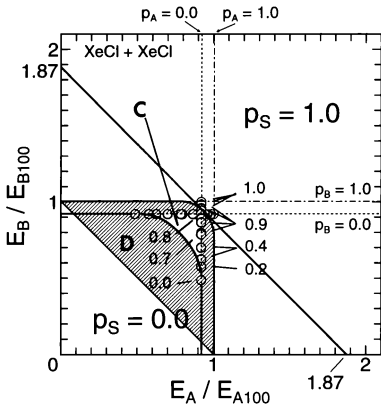


Fig. 2.11: Optical air breakdown probability p_S superposing two XeCl laser beams is mapped on a normalized energy plane. Each axis is normalized by the value of the threshold energy when each beam's air breakdown probability p_A or p_B becomes 1.00 (100%). The area C shows that an optical air breakdown can be produced by superposing two XeCl laser beams which can not produce an optical air breakdown separately. The area D shows the energy loss.

tion of XeCl laser beams seems to be caused by the oscillation time lag between the two XeCl lasers.

The optical air breakdown probability p_B versus the oscillation time lag τ between two XeCl lasers is shown in Fig. 2.12. In this experiment, the energy of both laser beams was below the threshold value of air breakdown by only one beam, i.e. $E_A, E_B < E_0$. This result shows that it is possible to produce an optical breakdown even when the time lag is over 100nsec. Since this time lag is longer than the XeCl laser oscillation, and since a XeCl laser beam produces weak ionization on its path near the focal point as shown in Chapter 5 and the previous paper¹⁵, the weakly ionized part seems to remain over 100nsec. This may lead to the reduction of the CO₂ laser energy required to form a plasma in the superposition of a CO₂ laser and a XeCl laser.

In Fig. 2.13, the breakdown probability p_B , when two wavelength laser beams (a CO₂ laser and a XeCl laser) were superposed simultaneously, is mapped on an energy plane. The open circle means $p_B = 1.0$, and the closed circle means $p_B = 0$. In this experiment, the time difference τ was kept within the range from -20nsec to 20nsec. Figure 2.14 shows photographs of a plasma made by the superposition of the CO₂ laser and the XeCl laser. The combination of laser energies of each photograph is mapped as the cross symbol with Roman numerals in Fig. 2.13. These results show that volume size of the plasma formed by superposing the CO₂ laser beam (750mJ) and the XeCl laser beam (38mJ) is about 800 times as big as that formed by only the XeCl laser beam (74mJ), though superposed energy is only about 10 times the energy of the single focused XeCl laser beam. As shown in Fig. 2.13, $E_C + 36.8E_X = 2200$ (when $E_X > 50\text{mJ}$) was obtained as an empirical equation. These results and this equation show that the superposition of a low energy XeCl laser beam on a CO₂ laser beam reduces drastically the required energy of the CO₂ laser beam for plasma formation.

Figure 2.15 shows the relation between the oscillation time lag τ and the number of successes and failures in plasma formation in the combination of the CO₂ laser beam and the XeCl

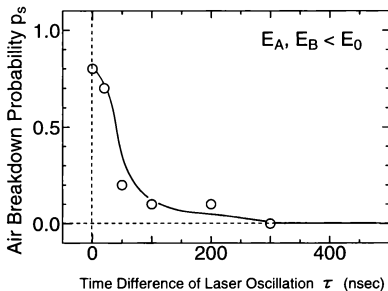


Fig. 2.12: The optical air breakdown probability p_s versus oscillation time lag τ between two XeCl lasers.

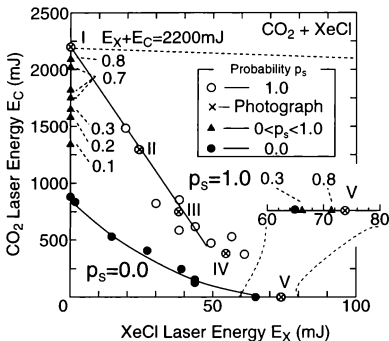


Fig. 2.13: The optical air breakdown probability p_s superposing a CO₂ laser beam and a XeCl laser beam is mapped on the energy plane. The horizontal axis is the XeCl laser energy, and the vertical axis is the CO₂ laser energy. The open circle means $p_s = 1.0$, and the closed circle means $p_s = 0$. The cross symbol with a Roman numeral shows the laser energy combination of each photograph shown in Fig. 2.14.

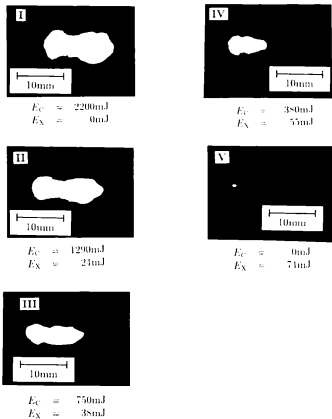


Fig. 2.14: Photographs of an optical air breakdown plasma made by superposing a XeCl laser beam and a CO_2 laser beam. The combination of the energies of a CO_2 laser and a XeCl laser for each photograph is mapped in Fig. 2.13.

laser beam. This figure shows that a plasma can be formed within the range of time lag $-85 < \tau < 75$ nsec, and that the time lag should be within $-35 < \tau < 20$ nsec in order to form a plasma without failure. The pulse shape and the timing of two laser beams are shown in Fig. 2.16(a) for shorter time lag and in (b) for longer time lag. As shown in Fig. 2.16(a), the XeCl laser pulse should be superposed on the spike part of the CO₂ laser pulse, i.e. $-35 < \tau < 20$ nsec, in order to form a plasma without failure. When the XeCl laser is oscillated after the CO₂ laser, a plasma can be formed so long as the XeCl laser pulse is in the tail part of the CO₂ laser pulse as shown in Fig. 2.16(b). On the other hand, when the XeCl laser is oscillated earlier than the CO₂ laser, a plasma formation can be done without overlap of laser pulses. In this case, the time lag is allowed up to 75 nsec. This is close to the allowed time lag in the combination of two XeCl lasers. These results show that the seed electrons produced by the XeCl laser, which have more than 100 nsec of life time, are heated up and led to a breakdown by the CO₂ laser pulse.

2.3.3 Discussion

The photon energy of a XeCl laser (4.03 eV) is much higher than that of a CO₂ laser (0.117 eV). The pulse shape of the CO₂ laser has a long tail part lasting about 2.5 μ sec and this part supplies much more than 2/3 of the total energy of the CO₂ laser, and the total energy of the CO₂ laser is much higher than that of the XeCl laser. As already reported¹⁵⁾ by the author and as shown in Chapter 5, a XeCl laser produces a weak ionization of about 10 mm length along its light path around the focal point. On the other hand, a CO₂ laser forms only a breakdown plasma and never does weak ionization. These results show that as compared with a CO₂ laser, a XeCl laser is much more effective for exciting atoms and molecules and for producing seed electrons by the multiphoton excitation and ionization because of its high photon energy. On the other hand, in comparison with a XeCl laser, a CO₂ laser pulse is much more effective for producing

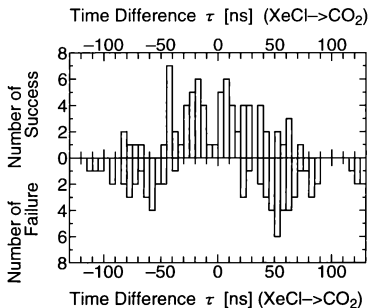


Fig. 2.15: The numbers of successes and failures in producing an optical air breakdown by superposing a CO₂ laser beam and a XeCl laser beam versus the delay time of laser oscillation from XeCl laser to CO₂ laser τ .

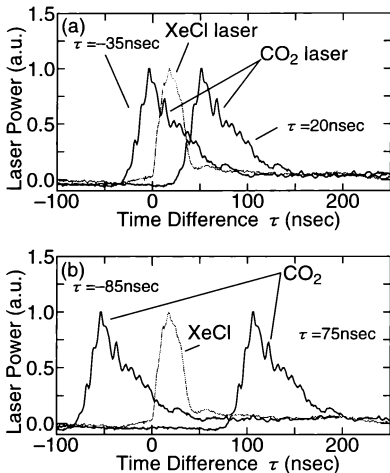


Fig. 2.16: The optical wave shape of a CO₂ laser and a XeCl laser. (a) Time difference τ is -35 nsec and 20 nsec. They are upper limits for plasma formation without failure. (b) Time difference τ is -85 nsec and 75 nsec. They are the limits for plasma formation.

and heating a breakdown plasma by the field acceleration because of its high electric field and high energy. So seed electrons seem to be made from a tiny particle and to be ionized by a CO_2 laser beam when only a CO_2 laser is used.

In the long plasma channel formation by a CO_2 laser beam, the channel consists of series of beads-like plasmas. They seem to be made by thermal heating of aerosols or tiny particles in the air. So the mechanism of plasma formation by a CO_2 laser may differ between long channel formation and these experiments. However, the superposition of laser beams is expected to form the high quality plasma channel which is one continuous plasma, because as shown in Fig.2.14 the length of the plasma along the CO_2 laser light path is kept though the CO_2 laser energy decreases at the superposition of the CO_2 laser and the XeCl laser .

In the superposition of a XeCl laser and a CO_2 laser, since a XeCl laser provides seed electrons which remain more than 100nsec, the threshold value of the CO_2 laser energy for plasma formation is drastically reduced and its energy is efficiently used for enlarging the volume size of the plasma. Thus the combination of a CO_2 laser and a XeCl laser achieves the efficient plasma formation.

2.4 Summary

Plasma formation by the superposition of laser beams was studied. Three combinations of superposition were tried, CO_2 - CO_2 , XeCl - XeCl , and CO_2 - XeCl . The experiments and numerical calculation were carried out in order to show that a plasma can be formed by superposition of laser beams, moreover in order to estimate the influences of the incident angle made by laser beams, of the time lag between them, and of the distance between focal points between them.

These results have been obtained. It has been made clear that an optical breakdown is produced by superposing two laser beams, the energy of which are both limited below the threshold value of a breakdown so as not to produce a breakdown by focusing only one beam.

The addition law of energy for plasma formation by superposition of laser beams of the same wavelength holds taking account of timing, positioning, and volume size of cross focusing of laser pulses.

The superposition of a CO_2 laser beam and a XeCl laser beam with fine tuning of timing and positioning reduces drastically the required energy of the CO_2 laser for plasma formation keeping the volume size of the plasma almost same as that formed by only a CO_2 laser. Thus, the combination of a CO_2 laser and a XeCl laser is effective for plasma formation because a XeCl laser produces seed electrons by its high photon energy and a CO_2 laser heats them up and leads them to a plasma by its high field and high energy.

Since the addition law of energy holds in the superposition of laser beams, the required energy of each one beam for plasma formation will be reduced by superposing many beams so long as they are simultaneously focused on the same point. So, a plasma formation by superposition of laser beams will be useful for Laser Triggering of Lightning.

References

- [1] P. D. Maker, R. W. Terhune and C. M. Savage : "Optical Third Harmonic Generation", *Quantum Electronics proceedings of the third international congress*, Vol.2, 1559-1576 (1963)
- [2] R. W. Minck : "Optical Frequency Electrical Discharges in Gases", *J. Appl. Phys.*, **34**, 252-254 (1964)
- [3] R. G. Meyerand, Jr. and A. F. Haught : "GAS BREAKDOWN AT OPTICAL FREQUENCIES", *Phys. Rev. Lett.*, **11**, 401-403 (1963)
- [4] R. G. Meyerand, Jr. and A. F. Haught : "OPTICAL-ENERGY ABSORPTION AND HIGH-DENSITY PLASMA PRODUCTION", *Phys. Rev. Lett.*, **13**, 7-9 (1964)
- [5] R. G. Tomlinson, E. K. Damon and H. T. Buscher : "PHYSICS OF QUANTUM ELECTRONICS Conference Proceedings (The Breakdown of Noble and Atmospheric Gases by Ruby and Neodymium Laser Pulses)", McGRAW-HILL BOOK COMPANY, pp.520-526 (1966)
- [6] R. W. Minck and W. G. Rado : "PHYSICS OF QUANTUM ELECTRONICS Conference Proceedings (Investigation of Optical Frequency Breakdown Phenomena)", McGRAW-HILL BOOK COMPANY, pp.527-537 (1966)

- [7] A. F. Haught, R. G. Meyerand, Jr. and D. C. Smith : "PHYSICS OF QUANTUM ELECTRONICS Conference Proceedings (Electrical Breakdown of Gases by Optical Frequency Radiation)", McGRAW-HILL BOOK COMPANY, pp.509-519 (1966)
- [8] D. H. Gill and A. A. Dougal : "BREAKDOWN MINIMA DUE TO ELECTRON-IMPACT IONIZATION IN SUPER-HIGH-PRESSURE GASES IRRADIATED BY A FOCUSED GIANT-PULSE LASER", *Phys. Rev. Lett.*, **15**, 845-847 (1965)
- [9] H. T. Buscher, R. G. Tomlinson and E. K. Damon : "FREQUENCY DEPENDENCE OF OPTICALLY INDUCED GAS BREAKDOWN", *Phys. Rev. Lett.*, **15**, 847-849 (1965)
- [10] C. Barthélemy, M. Leblanc and M. Boucault : "Variation du seuil de claquage de l'air en fonction de la longueur d'onde de l'irradiation laser", *COMPTES RENDUS HEBDOMADAIRES DES SÉANCES DEL'ACADÉMIE DES SCIENCES B(Paris)*, **266B**, 1234-1235 (1968)
- [11] A. J. Alcock, C. DeMicelis and M. C. Richardson : "WAVELENGTH DEPENDENCE OF LASER-INDUCED GAS BREAKDOWN USING DYE LASERS", *Appl. Phys. Lett.*, **15**, 72-73 (1969)
- [12] S. Yoshida, J. Sasaki, Y. Arai, M. P. Lei, K. Tateishi and T. Uchiyama : "Effect of UV preionization on optical breakdown induced by a pulsed CO₂ laser", *J. Appl. Phys.*, **58**, 620-622 (1985)
- [13] S. Yoshida, J. Sasaki, Y. Arai, and T. Uchiyama : "Effect of UV laser preionization on CO₂-laser-induced optical breakdown", *J. Appl. Phys.*, **58**, 4003-4005 (1985)
- [14] M. Kubo, R. Itatani, and S. Matsumura : "Basic Research for Laser Triggered Lightning Influence of Wavelength of Laser on Atmospheric Spark Discharge", *Trans. I.E.E.J.*, **112A**, 620-628 (1992)

- [15] M. Jinno, M. Kubo, and R. Itatani : "Triggering Discharge and Guiding Discharge Path by Weak Ionized Channel with Different Wavelength Laser Beams", *Trans. I.E.E.J.*, **115A**, 595-604 (1995)
- [16] M. Jinno, M. Kubo, and R. Itatani : "Steady-state Plasma Formation and Heating in the Open Air by Superposition of Microwave and XeCl Laser", *Trans. I.E.E.J.*, **116A**, 446-452 (1996)

Chapter 3

Plasma Formation by Superposition of a Laser Beam and a Microwave

3.1 Introduction

In recent years there has been a growing interest in Laser Triggering of Lightning due to the development of high power lasers. Many researchers have started studies on Laser Triggering of Lightning. The method using a laser-produced plasma channel¹⁻⁵⁾ and that using a weakly ionized channel⁶⁾ were proposed.

The method using a plasma channel produced by a single laser beam has a fatal problem, i.e. the plasma channel protects itself from expanding due to absorption and reflection of laser energy by the plasma channel itself. As the resolution of this problem the author's group proposed the Cross-Beam Method^{7,8)}. In this method, different wave lengths of laser beams can be used. In Chapter 2, the combination of UV laser and IR laser is examined and the effectiveness of it is shown using a CO₂ laser and a XeCl laser. On the other hand the combination of a laser beam and a microwave was proposed by Shindo⁹⁾. The combination of a UV laser and a microwave is expected to be effective for plasma formation because of the effectiveness of the combination of a UV and an IR laser beams and this combination was

proposed by the author's group^{10,11}. Since DC operation is much easier for microwaves than for lasers, a microwave is expected to lead seed electrons, which are made by a UV laser, to a steady-state plasma. Moreover, since the air transmits a microwave with low loss, a microwave will be useful for Laser Triggering of Lightning.

The ozone layer protection by resolution of Freon using a plasma which is produced in the troposphere by a microwave was proposed¹². Since the superposition of a microwave and a laser beam seems to reduce the required power of a microwave for plasma formation from the power required when only a microwave is used, the superposition of a microwave and a laser beam is expected to be effective for the ozone layer protection by a plasma.

The reduction of the optical breakdown threshold in inert gases, the pressure of which are below 500mHg, due to the superposition of a laser beam and a microwave was reported¹³. The reduction of the optical breakdown threshold versus gas pressure was theoretically discussed^{14,15}. The plasma production due to microwave discharge is studied using electrodes in the waveguide in the hydrogen atmosphere¹⁶. However, there is no report about plasma formation in the open air by superposition of a microwave and a laser beam.

In this chapter, the experiments of plasma formation by superposition of a microwave and a XeCl laser beam are described, and the reduction of the breakdown threshold is discussed using a microwave equivalent circuit.

3.2 Experimental Setup

A schematic diagram of the microwave circuit is shown in Fig. 3.1. The maximum output power of the magnetron (IMG-2502-S Tokyo Denshi Co. Ltd.) is 1.5kW at the frequency of 2.45GHz. The power monitor (IMM-2502-S Tokyo Denshi Co. Ltd.) and the isolater (IEF-1202I Tokyo Denshi Co. Ltd.) were used. Since the anode current of the magnetron $I(A)$ and the output power of the magnetron $P(W)$ has the relation of $P = 2.72 \times 10^3 I$, the output power is measured

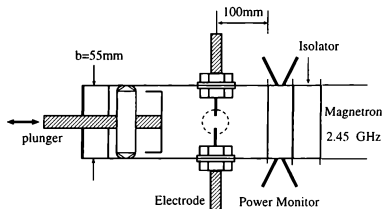


Fig. 3.1: Schematic diagram of a microwave circuit.

by checking the anode current through the experiments. The rectangular waveguide is made of aluminum and its width is 1.09×10^2 mm, height is 55.0mm. The distance from the end of the power monitor to the electrodes is 100mm. Since the cross section of the waveguide is 60.0cm^2 , the power density of the microwave injected into the waveguide is $16.7\text{W}/\text{cm}^2$ per 1kW output of the magnetron. However, in order to calculate the power density between the electrodes, it is necessary to take account of the multi reflections in the waveguide as discussed in section 3.4. Thus the intensity of the microwave is estimated by the power injected into the waveguide.

The electrodes are made of tungsten rod and brass bolt. The diameter of the tungsten part is 3mm. They are installed on the E plane of the waveguide facing each other with 3mm of the distance. The tungsten rod is welded to the brass bolt. This bolt is fixed to the waveguide by the brass nuts. The end of the waveguide is terminated by the movable plunger in order to adjust the position of the standing wave. The waveguide has a round hole of 1cm diameter on the side wall for laser injection and has a mesh window made of copper on the other side wall for observation. All of the experiments are carried out in the open air in the laboratory. The room temperature is kept at 20-25°C, and the humidity is kept at 60-80%. In these ranges, the plasma formation receives no influence.

Table 3.1 shows the characteristics of the XeCl laser. The XeCl laser beam was focused by the quartz lens ($f=475\text{mm}$, $\phi = 50\text{mm}$). The experimental setup is shown in Fig. 3.2. The XeCl laser beam is focused on the center of the gap between electrodes by the lens. The energy of the laser beam is controlled by the aperture set on the laser light path. The energy coming out from the lens is measured by the Joule meter (J-50 Molelectron). Since the diameter of the focal spot measured from the burn pattern on thermal paper is 1.2mm, the energy density of the laser beam on the focal plane is calculated as $6\text{J}/\text{cm}^2$ when the output energy of laser beam is 100mJ. However, the burn pattern becomes larger than the real spot size of the laser beam because a plasma is produced on thermal paper. Then it is difficult to measure accurately the

Table 3.1: Characteristics of the XeCl excimer laser.

Wavelength	308nm
Max. Output Energy	400mJ
Peak Power	13.3MW
F.W.H.M.	25nsec
Power Fluctuation	$\pm 2.5\%$

spot size of the laser beam. The optical intensity of the laser beam is not uniform in the beam. So, the intensity of the XeCl laser beam at the focal plane is estimated by the output energy of the laser beam.

The laser pulse is detected by the photo-tube (R1193-U05 HAMAMATSU). The reflected microwave is detected by the power monitor. Then the delay time from the laser injection to plasma formation is obtained from them. The plasma formation process is recorded to the VTR through the mesh window.

The plasma formation and heating were tried in the three cases: microwave only, XeCl laser beam only, and superposition of a microwave and a XeCl laser beam.

3.3 Experimental Results

3.3.1 Plasma Formation by Microwave

The plunger was set to the position where the radiation from a small neon discharge lamp becomes maximum. This neon discharge lamp was set near the electrodes. In all the experiments the plunger was set to this position. After setting the plunger, the neon tube was taken away. Though the plasma formation was examined at the maximum microwave power, no plasma was formed because of the low intensity of the electric field between the electrodes as described in section 3.4.

3.3.2 Plasma Formation by XeCl laser

In Fig.3.3, a photograph of a plasma produced by a XeCl laser, and its sketch are shown. The output energy of the XeCl laser was 85mJ. The air breakdown probability versus the XeCl laser energy is shown in Fig.3.4. The probability was obtained by 10 tries at each energy. The probability curve has the threshold energy value E_{th} of 55mJ.

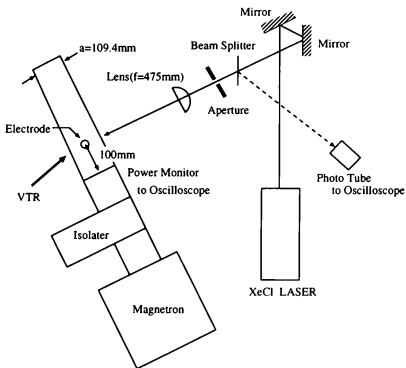


Fig. 3.2: Experimental setup for superposition of a microwave and a XeCl laser beam.

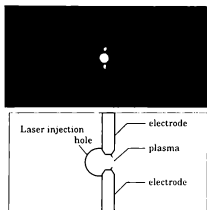


Fig. 3.3: A plasma formed by a XeCl laser. (Upper: Photo, Lower: Sketch)

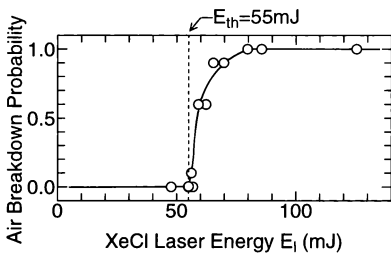


Fig. 3.4: Air breakdown probability vs XeCl laser energy.

3.3.3 Plasma Formation by the Superposition of Microwave and XeCl laser

Figure 3.5 shows the VTR photographs of the process of plasma formation by superposition of a microwave and a XeCl laser. Moreover Fig. 3.5 shows the sketch of the first field of VTR photograph. At that time the energy of the XeCl laser was 47mJ, which is below the threshold value, and the microwave input power was 1.5kW, then neither laser nor microwave produce a plasma respectively. The first field shows that a dot-like plasma is produced at the focal point of the XeCl laser beam between electrodes by superposition of the microwave and the XeCl laser. In the next field, the dot-like plasma changes into a steady-state glow discharge plasma.

Figure 3.6 shows the time dependence of the reflected microwave power after laser injection. Since the laser energy was 50mJ which is below the breakdown threshold energy, a plasma is never formed by only laser beams. The change in reflected power after laser injection means the microwave absorption by the plasma. This figure shows that small absorption occurs during several tens of μsec after τ sec from laser injection then large absorption occurs and it becomes steady-state. In Fig.3.7, the delay time of absorption versus microwave input power is shown. The empirical equations of delay time $\tau_{\text{off}}(\mu\text{sec})$ and $\tau_{\text{on}}(\mu\text{sec})$ are obtained from this figure as follows,

$$\tau_{\text{off}} = 23.5e^{-1.51P} \quad (3.1)$$

$$\tau_{\text{on}} = 3.00e^{-0.736P} \quad (3.2)$$

Where $P(\text{kW})$ is the input power of microwave, $\tau_{\text{off}}(\mu\text{sec})$ is the delay time when the laser energy is below the breakdown threshold energy ($E_L = 50\text{mJ}$) and $\tau_{\text{on}}(\mu\text{sec})$ is that when the laser energy is over the threshold energy ($E_L = 110\text{mJ}$). These results show that the first small absorption seems to be caused by the plasma formed between electrodes, and that the later large absorption seems to be caused by the steady-state plasma which spreads in the waveguide. τ_{on} is the time from laser injection to the absorption by the laser-produced plasma between electrodes.

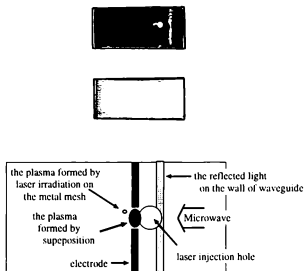


Fig. 3.5: VTR photographs of plasma formation by superposition of a microwave and a XeCl laser. $E_t = 17 \text{ mJ}$, $P = 1.5 \text{ kW}$ (Upper: 1st field, Middle: 2nd field, Lower: Schematics of 1st field)

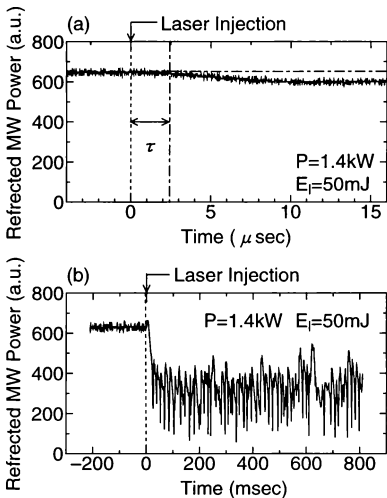


Fig. 3.6: Waveforms of reflected microwave power.

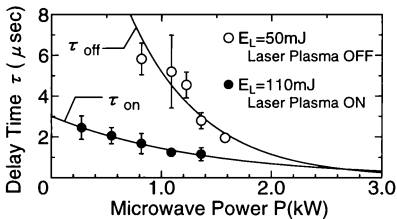


Fig. 3.7: Delay time of microwave absorption vs microwave power.

τ_{off} is the time from laser injection to the absorption by the weakly ionized part⁽⁶⁾ produced by the XeCl laser between electrodes. Then, the time lag between τ_{off} and τ_{on} seems to be the time of plasma formation by superposition of the microwave and the XeCl laser.

In Fig. 3.8, the steady-state plasma formation probability p versus the microwave input power P (kW) is plotted. The probability was obtained by 10 tries at each point. Figure 3.8(a) is the result when the energy of the XeCl laser is below the breakdown threshold energy, and (b) is that when the laser energy is over the threshold energy. In both (a) and (b), the probability increases when the laser energy or the microwave power increases.

From these results, the microwave input power required for producing a steady-state plasma at $p=0.5$ and 1.0 for each laser energy are obtained and plotted in the Fig. 3.9. All the three curves leap at the same laser energy. Since this threshold is the same as the breakdown threshold of a XeCl laser, the curves are divided into two parts whether the seed plasma is produced or not. When the seed plasma is produced by the XeCl laser, the required power of the microwave is drastically reduced. Then, the required power of the microwave for plasma heating seems to be lower than that for plasma formation. The superposition of the XeCl laser and the microwave reduces the required energy of the XeCl laser for plasma formation from 55mJ to 10mJ. So, the effect of superposition of the XeCl laser and the microwave on plasma formation and heating is clarified.

3.4 Discussion

The electrodes with nuts, the gap between electrodes and the waveguide are treated respectively as inductance L , capacitance C and transmission line whose characteristic impedance is Z_0 . Then the electric field between electrodes is calculated on the equivalent circuit shown in Fig. 3.10, where L_N is the inductance of the nut, L_W is the inductance of the tungsten rod.

Since the length of the long side of the rectangular waveguide a is 1.09×10^2 mm and that

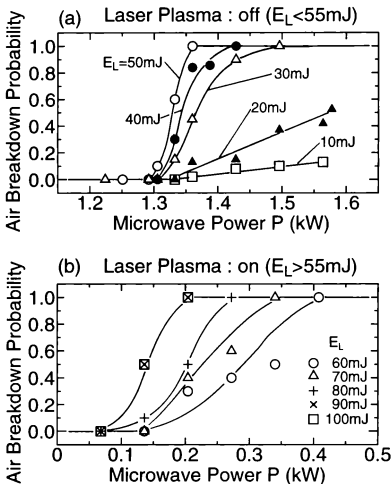


Fig. 3.8: Air breakdown probability vs microwave power.

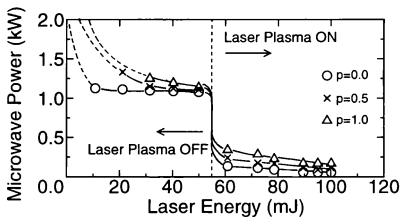


Fig. 3.9: Condition of XeCl laser energy and microwave power for plasma formation.

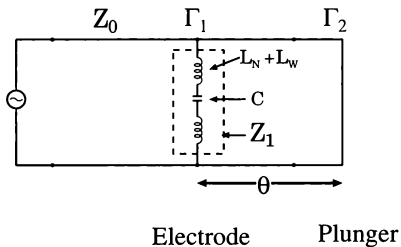


Fig. 3.10: Microwave equivalent circuit.

of the short side b is 55mm, the mode of the microwave is TE_{10} in the waveguide. Since in the air, $\epsilon \simeq \epsilon_0$ and $\mu \simeq \mu_0$ hold, the characteristic impedance Z_0 is given as follows¹⁷⁾,

$$Z_0 = \frac{2b}{a} \frac{\lambda_2}{\lambda} \sqrt{\frac{\mu}{\epsilon}} \simeq \frac{4b}{\sqrt{1a^2 - \lambda^2}} \sqrt{\frac{\mu_0}{\epsilon_0}}, \quad (3.3)$$

where $\lambda_2(m)$ is the wavelength of the microwave in the waveguide. Since the wavelength is given as $\lambda = 12.2\text{cm}$, the impedance is given as $Z_0 = 4.57 \times 10^4 \Omega$.

The inductance L of a rod conductor, whose length is l and radius is R , is given as^{18,19)},

$$L = 2 \int_0^R \int_0^R \frac{L(r, r') 4rr' dr' dr}{R^4}, \quad (3.4)$$

where

$$L(r, r') = \frac{\mu}{4\pi} \frac{1}{2\pi} \int_0^{2\pi} \int_0^l \int_0^l \frac{dz dz' d\theta}{\sqrt{(z - z')^2 + r^2 + r'^2 - 2rr' \cos \theta}}.$$

Then the inductances of the nut part L_N ($R = 6.30\text{mm}$, $l = 11.0\text{mm}$) and the tungsten rod part L_W ($R = 1.50\text{mm}$, $l = 15.0\text{mm}$) are respectively calculated as follows, $L_N = 2.08\text{nH}$ and $L_W = 6.74\text{nH}$. So, the inductance of electrodes L is calculated, $L = 2 \times (L_W + L_N) = 17.6\text{nH}$. On the other hand, the capacitance of the gap C is determined by using the charge simulation method²⁰⁾ as $C = 3.79\text{pF}$.

Though the voltage wave, which comes from the magnetron, is reflected partially by the electrodes, this reflected wave passes through the isolator and is absorbed by the dummy load. So, this reflected wave is neglected. On the other hand, the voltage wave, which passes out from the electrodes, is reflected perfectly by the plunger. Then the voltage wave causes multi-reflection between the plunger and the electrodes. So, in order to calculate the electric field between the electrodes, this multi-reflection should be accounted. The amplitude of the traveling voltage wave V at the electrodes is given as,

$$V = (1 + \Gamma_1)V_0 + \Gamma_2 \Gamma_1 e^{-\gamma 2l} V, \quad (3.5)$$

where V_0 is the amplitude of the incident voltage wave. θ is the electrical degree from electrodes to the plunger. Γ_1 is the voltage reflection coefficient at the electrodes, and Γ_2 is that at the plunger. The right hand first term of equation (3.5) is the transmitted voltage wave at the electrodes, and the second term is the traveling voltage wave reflected by the plunger and the electrodes. Since the plunger is a perfect reflector, $\Gamma_2 = -1$. The plunger is set to the position where θ becomes 1.5π so that the loop of the voltage standing wave should stand on the electrodes. The voltage reflection coefficient Γ_1 is given as follows²¹⁾.

$$\Gamma_1 = -\frac{Z_0}{Z_0 + 2Z_1}, \quad (3.6)$$

where Z_1 is the impedance of the electrodes, given as $Z_1 = j(\omega L - 1/(\omega C))$. The amplitude of the traveling voltage wave V at the electrodes is obtained as follows by solving the equation (3.5) for V using each value of Z_0, L, C .

$$V = (2.36 \times 10^{-1} + j4.25 \times 10^{-1})V_0. \quad (3.7)$$

The maximum value of electric field of TE₁₀ mode microwave in the waveguide E_{\max} (V/m) is given as follows²²⁾,

$$E_{\max} = \sqrt{\frac{8P}{b\sqrt{4a^2 - \lambda^2}} \sqrt{\frac{\mu_0}{\epsilon_0}}}, \quad (3.8)$$

where P (W) is the input power of the microwave. So, by substitution of each value to this equation, E_{\max} is obtained as $E_{\max} = 5.50 \times 10^2 \times \sqrt{P}$. Then the maximum value of the microwave electric field between the electrodes E_G (V/m) is written as.

$$E_G = \frac{b}{d} \frac{|V|}{|V_0|} E_{\max} = 4.90 \times 10^3 \sqrt{P}, \quad (3.9)$$

where b is the length of the short side of the waveguide, and d is the gap width.

The discharge electric field intensity of a rod-rod gap with 50Hz sin-wave voltage applied is 1.13×10^6 (V/m²³⁾. When the frequency of applied voltage becomes 2.45GHz of microwave range, the discharge field intensity is reduced to about 60% of that of 50Hz^{24, 25)}. Then the discharge

field intensity between the electrodes is obtained as $E_{BD} = 6.78 \times 10^5 \text{V/m}$. When $E_c > E_{BD}$ holds, a discharge occurs between the electrodes and a plasma is produced. So, the required microwave input power for plasma formation is obtained from equation (3.9) as $P = 19 \text{kW}$. Figure 3.9 shows that the microwave power required for steady-state plasma formation with 1.0 of probability is about 1.5kW when the XeCl laser beam, the energy of which is below the breakdown threshold, is superposed. So, by the superposition of the microwave and the XeCl laser beam, the required power of the microwave for steady-state plasma formation is reduced to 8% of that without laser superposition. On the other hand, as described in Chapter 2, the superposition of the CO_2 laser and the XeCl laser gives a 30% reduction of the required energy of the CO_2 laser for plasma formation. These results show that the superposition of a microwave and a XeCl laser is much more effective.

Here, let us discuss about field acceleration. The electron-ion collision frequency ν is given as follows;

$$\nu = n\sigma\bar{v} \simeq n\bar{v}\pi r^2, \quad (3.10)$$

where n is the density of neutral particles, σ is the momentum transfer cross-section, \bar{v} is the thermal velocity of the electrons, and r is the radius of the particle. The density n at 20°C is given as $n \simeq 3.56 \times 10^{16} p(\text{cm}^{-3})$, where $p(\text{Torr})$ is the pressure of the gas. The velocity \bar{v} is given as $\bar{v} = 6.7 \times 10^7 \sqrt{T_e}(\text{cm/sec})$, where $T_e(\text{eV})$ is the electron temperature. Since all the experiments in Chapter 2 and 3 were carried out in the open air, the pressure p is 760Torr. Since the radius of the particle (air i.e. the mixture of N_2 and O_2) is $r \simeq 1.8 \times 10^{-8} \text{cm}^{26}$, the collision frequency ν is given by

$$\nu \simeq 1.8 \times 10^{12} \sqrt{T_e}(\text{Hz}). \quad (3.11)$$

The electron temperature of a laser-produced plasma is about $1 \sim 10 \text{eV}^{27}$. So, when the seed electrons are produced by the XeCl laser, the electron temperature T_e seems to be higher than $2.5 \times 10^{-2} \text{eV} (\simeq 300\text{K})$ and lower than 1eV . Then the collision frequency of seed electrons is

calculated as $3 \times 10^4 \text{GHz}$ (for $T_e = 2.5 \times 10^{-2} \text{eV}$) $< \nu < 1.8 \text{THz}$ (for $T_e = 1 \text{eV}$). A microwave of millimeter class is in this range, and approximately several hundreds GHz of microwave seems to be the most suitable for heating the seed electrons produced by the XeCl laser. The frequency of a CO_2 laser is 28THz , and that is too high. The frequency of the microwave used in the experiments is 2.45GHz . Then the collision frequency of seed electrons is closer to the frequency of the microwave than that of the CO_2 laser. So, the microwave of 2.45GHz seems to be more effective for field acceleration of seed electrons than the CO_2 laser. This seems to be the reason why the combination of a XeCl laser and a microwave is more effective than that of a XeCl laser and a CO_2 laser. On the other hand, in the case of the field acceleration of laser-produced plasma, the electron temperature T_e is in the region $1 \sim 10 \text{eV}$. So the collision frequency of the electrons in laser-produced plasma is in the region $1.8 \text{THz} \sim 6.0 \text{THz}$. This range is covered by the sub-millimeter microwave. From the viewpoint of collision frequency of electron, CO_2 laser is much more suitable for plasma heating than the heating of the seed electrons.

3.5 Summary

The steady-state plasma formation by superposition of a microwave and a XeCl laser is achieved. Both of them can not produce a plasma respectively, is achieved. The superposition of a microwave and a XeCl laser reduces the breakdown threshold of the microwave electric field to 8% of that by only the microwave. On the other hand, the required energy of the XeCl laser is reduced to 20% by the superposition of the microwave. It is shown that a microwave heats a plasma, which is made by the superposition, and leads the plasma to the steady-state. Especially, the microwave of centimeter class or millimeter class is suitable for acceleration of seed electrons by its field. On the other hand, the IR laser and the sub-millimeter class microwave are suitable for plasma heating by their field.

Considering Laser Triggering of Lightning, when the triggering is done by a pulsed laser, the laser should be oscillated just before the rising of electric field up to the breakdown intensity. However, the superposition of a microwave and a laser beam produces a steady-state plasma, and it becomes possible to wait for the rise of the electric field after plasma formation. Thus the superposition of a microwave and a laser beam is effective for plasma formation and heating. Moreover, the superposition of them is expected to be applied to ozone protection by a plasma.

References

- [1] T. Uchiyama, M. Hirohashi, H. Miyata and T. Sakai : "Study of Triggering Lightning by using TEA CO₂ Laser", *Rev. Laser Eng.*, **16**, 267-277 (1988) [in Japanese]
- [2] T. Shindo, Y. Aihara, M. Miki and J. Wada : "Theoretical study of laser-triggered lightning (Pt. 1) - Calculation of plasma production by a laser -". *CRIEPI Report.No. T91057* (1992) [in Japanese]
- [3] T. Shindo, Y. Aihara, M. Miki and T. Suzuki : "Model Experiments of Laser Triggered Lightning", *IEE Transactions on Power Delivery*, **8**, 311-317 (1993)
- [4] C. Honda, T. Takuma, K. Muraoka, M. Akazaki, F. Kinoshita and O. Katahira : "Characteristics of Discharge Induced by Laser-Generated Plasmas". *Trans. I.E.E.J.*, **113-B**, 994-1002 (1994) [in Japanese]
- [5] T. Uchiyama : "Laser Triggering Lightning", *Jpn. J. Plasma and Fusion*, **70**, 168-172 (1994) [in Japanese]
- [6] K. Nakamura, T. Suzuki, C. Yamabe and K. Horii : "Fundamental Research for Lightning Trigger Experiment by Using UV Lasers". *Trans. I.E.E.J.*, **113-B**, 1265-1273 (1993) [in Japanese]

- [7] M. Kubo, K. Okayama, A. Taketani, N. Kosugi and R. Itatani : "The effect of simultaneous irradiation of laser beams on triggering discharge". *1989 National Convention Records of I.E.E.J.*, No. 111 (1989) [in Japanese]
- [8] M. Jinno, M. Kubo, and R. Itatani : "Triggering Discharge and Guiding Discharge Path by Weak Ionized Channel with Different Wavelength Laser Beams", *Trans. I.E.E.J.*, **115A**, 595-604 (1995) [in Japanese]
- [9] T. Shindo, T. Suzuki : "Laser-induced gas breakdown and its application for lightning protection", *The report of CRIEPI*, No. 182010 (1982) [in Japanese]
- [10] M. Jinno, T. Kishi, M. Kubo and R. Itatani : "The fundamental research on laser triggering of lightning XIV - The plasma formation by superposition of microwave and laser beam -", *I.E.E.J. Papers of ED*, **ED-94-145** (1994) [in Japanese]
- [11] M. Jinno, T. Kishi, M. Kubo and R. Itatani : "The fundamental research on laser triggering of lightning XVI - The plasma formation and heating by superposition of microwave and laser beam -", *I.E.E.J. Papers of ED*, **ED-95-77** (1995) [in Japanese]
- [12] G. A. Askar'yan, G. M. Batanov, A. É. Barkhudarov, S. I. Gritsinin, E. G. Korchagina, I. A. Kossyĭ, V. P. Silakov and N. M. Tarasova : "Electron attachment explodes Freon molecules: New possibilities for removing Freons from the atmosphere". *JETP Letters*, **55**, 515-520 (1992)
- [13] A. P. Darmanyany, V. E. Mitsuk and V. A. Chernikov : "LOWERING OF THE OPTICAL BREAKDOWN THRESHOLD IN A LASER FOCUS BY SUPERIMPOSING A MICROWAVE FIELD". *JETP Letters*, **8**, 71-74 (1968)
- [14] I. E. Poyurovskaya : "Gas breakdown by combined laser and microwave irradiation". *Sov. Phys. Tech. Phys.*, **21**, 729-731 (1976)

- [15] Robert W. Schmieder : "Pressure dependence of gas breakdown by combined laser and microwave fields", *J. Appl. Phys.*, **50(2)**, 712-725 (1979)
- [16] M. Kando : "Processing plasma production due to microwave discharges promoted by use of electrodes", *Report on Control of Reactive Plasmas (Grant-in-Aid for Scientific Research on Priority Areas Ministry of Education, Science and Culture)*, pp.464-469 (1992)
- [17] K. Funayama : "Kaisetsu-Maikuroha-gijyutsu (Microwave Engineering)", Denki-Shoin (1972) [in Japanese]
- [18] J. U'moto : "Denjiki-Gaku (Electro-Magnetics)", Syoko-do (1991) [in Japanese]
- [19] H. Takahashi : "Denjiki-Gaku (Electro-Magnetics)", Syoka-bou (1972) [in Japanese]
- [20] T. Kouno and T. Takuma : "Suuchi-Denkai-Keisan-Hou (Numerical Calculation of Electric Field)", Korona-Sha (1987) [in Japanese]
- [21] B. Oguchi : "Maikuroha-oyobi-Miriha-Kairo (Circuits of Microwave and Miriwave)", Maruzen (1964)
- [22] T. Makimoto : "Maikuroha-Kougaku-no-Kiso (Basics of Microwave Engineering)", Hirokawa-shoten (1972)
- [23] Y. Nakano : "Koudenatsu-Kougaku (High voltage Engineering)", Ohm-sha (1966)
- [24] I.E.E.J. : "Houden-Hand-Book (Electrical Discharge Handbook)", I.E.E.J. (1975)
- [25] Y. Karasuyama : "Koudenatsu-Kougaku (High voltage Engineering)", Corona-sha (1960)
- [26] Earl W. McDaniel : "Collision Phenomena in Ionized Gases", John Wiley & Sons Inc. (1964)

- [27] M. M. Litvak and David F. Eddwards : "Electron recombination laser-produced hydrogen plasma", *J. Appl. Phys.*, **37**, 4462-4474 (1966)

Chapter 4

Triggering an Electrical Discharge by a Laser Produced Plasma

4.1 Introduction

In the Laser Triggered Spark Gap(LTSG), a discharge is triggered by a metal vaporized plasma made by laser irradiation of an electrode. There are many reports of its mechanism¹⁻³⁾. It was reported that the delay time of discharge is varied by electron attachment to neutral particles in a uniform field gap⁴⁾, however the negative ion was never identified.

After the first report of the Laser Lightning Rod System by Ball in 1974⁵⁾, the gap distance of LTSG has been expanded and many researches have been done as the fundamental research for Laser Triggering of Lightning⁶⁻⁹⁾. The author's group proposed Cross-Beam Laser Triggering of Lightning¹⁰⁾. They have studied triggering and guiding an electrical discharge by ball-shaped plasmas produced by laser beams free from irradiation of electrodes.

In the experiments of triggering a discharge by a laser-produced plasma, they found that though a discharge is triggered by the plasma, the discharge path sometimes avoids the plasma¹¹⁻¹³⁾. After that, the same phenomenon was reported by the other group¹⁴⁻¹⁶⁾. However, the mechanism of this phenomenon has never been revealed.

In this chapter, the correlation between the path of discharge triggered by a laser-produced plasma and the discharge current is observed. Then the following result is obtained; When the discharge path avoids the laser-produced plasma, the current has more than two peaks before the flashover, on the other hand when the discharge path goes through the plasma, it has no peak between the first peak and the flashover. Moreover in this chapter, a flashover between the electrodes built in the chamber is triggered by a plasma produced by a XeCl laser beam on the midpoint between electrodes. The delay time of discharge versus the applied voltage between electrodes and versus the gas mixing ratio of oxygen and nitrogen filled in the chamber is investigated, from the viewpoint of clarifying the mechanism of triggering a discharge by a laser-produced plasma. Then it is shown that the delay time of discharge leaps between "late discharge" and "early discharge" at a certain voltage in the mixture containing oxygen. Moreover it is shown that the leap of the delay time is caused by the variation of the balance between electron attachment to oxygen and electron detachment from oxygen negative ions.

4.2 The Correlation between an Electrical Discharge Current and a Path of Electrical Discharge Triggered by a Laser Produced Plasma

In this section, the correlation between the discharge path and the discharge current is observed when a discharge is triggered by a XeCl laser-produced plasma. This is carried out as fundamental research on the trigger and guide effect of a laser-produced plasma on an electrical discharge.

4.2.1 Experimental Setup

The experimental setup is shown in Fig. 4.1. The XeCl laser (EXL-100S Nippon Denchi Co.

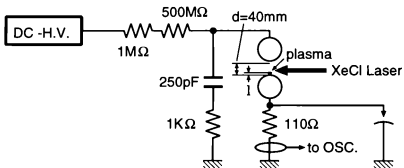


Fig. 4.1: Experimental setup for observing the discharge path and the discharge current.

Ltd.) was used. The laser pulse was detected by the photo tube (R1193-U05 HAMAMATSU). The discharge current was measured by the Rogowski Coil (model 2877 PEARSON ELECTRONICS Inc.) which was set on the earth line from the electrode. Spherical electrodes were used and they were made of stainless steel. Their diameters were 76mm and the gap distance was 40mm. One of the electrodes was earthed and the other had a DC negative voltage applied. Since the applied voltage was below the self breakdown voltage which is over 100kV, a flashover never occurred without laser-produced plasma. A plasma was produced by the XeCl laser beam which was focused by the quartz lens of 475mm focal length. The energy of the laser beam injected to the focal points was 130mJ which is sufficient for plasma formation. The plasma was produced on the axis of electrodes, 3mm from the anode according to the results of the experiments in Chapter 5, i.e. the plasma produced near the anode works effectively for triggering and guiding an electrical discharge. An electrical discharge was triggered in this system and the discharge path and the discharge current were observed.

4.2.2 Experimental Results and Discussion

An electrical discharge is triggered when the applied voltage V_g is over 55kV. In most of the trials at $V_g=55kV$ and 60kV, the discharge path goes through the plasma. When the applied voltage V_g is 70kV or 80kV, though the discharge path goes through the plasma in about 80% of trials, the path avoids the plasma in 20% of trials. In all the trials at $V_g=90kV$ and 100kV, the discharge path goes through the plasma and it becomes straight.

The current waveform at $V_g=80kV$ is shown in Fig. 4.2. The photographs of these discharges (cf. Fig.4.2) are shown in Fig. 4.3. In both Figs. 4.2 and 4.3, (a) is the discharge which goes through the plasma, and (b) is that avoiding the plasma. The photographs show that when the discharge path goes through the plasma, it is straight. Moreover it is shown that when the path avoids the plasma, the path bends at some points. When the discharge path goes through

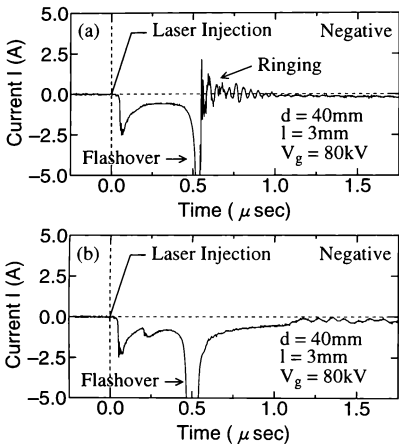


Fig. 1.2: Discharge current. (a) Discharge path goes through the plasma. (b) Discharge path avoids the plasma.

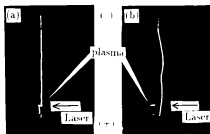


Fig. 1.3: Discharge triggered by a laser plasma. (a) Discharge path goes through the plasma. (b) Discharge path avoids the plasma.

the plasma, the current has a peak of several amperes immediately after the laser injection, then a current of about 1A flows and the flashover occurs as shown in Fig. 4.2(a). On the other hand, when the discharge path avoids the plasma, the current has the second peak between the first peak after laser injection and flashover as shown in Fig. 4.2(b).

At $V_g=80kV$, the discharge going through the plasma was observed 20 times and the current waveforms were the same as that shown in Fig.4.2(a) at all the trials. On the other hand, the discharge avoiding the plasma was observed 5 times and all of their current had the second peak between the first peak and the flashover the same as that of Fig. 4.2(b). Thus, there is a clear correlation between whether the discharge path goes through the plasma or not and the current waveform.

The shape of increase in the second current peak between the first peak and the flashover is different from that of flashover when the discharge path avoids the plasma. The discharge path bends at some points when it avoids the plasma. So, the triggering mechanism of discharge seems to be different when it goes through the plasma and when it avoids the plasma. For example, when the discharge avoids the plasma, such a mechanism seems to be probable as follows; the photodetachment from oxygen negative ion occurs¹²⁾ by UV light from the laser-produced plasma and the electron avalanche is formed at the point away from the plasma, then the discharge avoiding the plasma is formed. Otherwise, the discharge avoiding the plasma seems to be caused by the ionization of aerosol or some tiny particles between the electrodes.

Since this phenomenon seems to give much information for revealing the mechanism of triggered discharge by a laser-produced plasma, more work about this phenomenon is required.

4.3 The Effect of Oxygen on the Delay Time of Flashover Triggered by a Laser-Produced Plasma

In this section, an electrical discharge is triggered by a XeCl laser-produced plasma in the mixture of oxygen and nitrogen. The effect of oxygen on the jump of the delay time of discharge versus applied voltage between electrodes is observed and the mechanism of it is described.

4.3.1 Experimental Setup

The experimental setup is shown in Fig. 4.1. A plasma was produced by a XeCl laser beam on the midpoint between the stainless spherical electrodes. The electrodes were built in the stainless chamber. The laser beam was injected into the chamber perpendicularly to the axis of the electrodes through a quartz window and was focused by a quartz lens ($f=475\text{mm}$). The laser output energy was set to 100mJ which is sufficient to produce a plasma. The diameter of each electrode was 25mm. The distance between the electrodes, i.e. the gap distance d was 20mm. The positive DC high voltage was applied to one electrode, and the other electrode and the chamber were earthed.

Two apertures were set in the chamber in order to protect the electrodes from irradiation by the laser beam which induces photoemission from the electrodes. The laser pulse was detected by the phototube (R1193-U05, HAMAMATSU). The discharge current was detected by the current probe (A6303, TEKTRONICS) which was set on the earth line from the electrode. The chamber was filled with a mixture of oxygen and nitrogen. Their total pressure was kept at $1.0 \times 10^5 \text{Pa}$ (760Torr) and the mixing ratio was changed.

In this system, an electrical discharge was triggered by a laser-produced plasma. The delay time of discharge from laser injection was measured as a function of the applied voltage between the electrodes while changing the mixing ratio of the mixture.

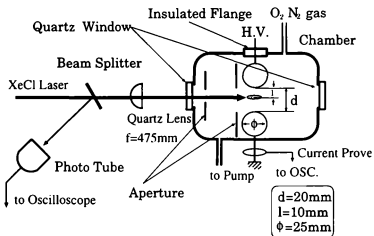


Fig. 1.1: Experimental setup for observation of the jump of delay time of discharge.

4.3.2 Experimental Results

The delay time of discharge τ_d versus the applied voltage V_k and versus the partial pressure of oxygen p_o is shown in Fig. 4.5. The delay time at each condition is measured more than 10 times, and the mean value of the delay time is plotted as a dotted circle. Each error-bar ($\pm\sigma$:standard deviation) is within each dotted circle. So, the statistic time lag is so short as to be neglected. Then the delay time is considered as the formative time lag. On the xy plane, V_0 (the minimum voltage of triggering a discharge) and V_{SBD} (the self breakdown voltage) are plotted.

In Fig. 4.6, the delay times τ_d versus the applied voltage V_k at each mixing ratio of the mixture are shown; $N_2:O_2 =$ (a)10:0, (b)7:3, (c)3:7, and (d)0:10. These figures show that as the applied voltage becomes higher, the delay time becomes shorter. Moreover they show that when oxygen exists in the mixture, the delay time becomes longer than that in nitrogen. The threshold of applied voltage V_{th} exists, and the delay time changes drastically by about one order of magnitude at V_{th} . Here, call the discharge at the lower applied voltage V_k ($V_k < V_{th}$) as "late discharge", and that at the higher applied voltage V_k ($V_{th} < V_k$) as "early discharge". Figure 4.6 shows that the leap of the delay time never occurs in nitrogen and in the mixture of low partial pressure of oxygen. Moreover Fig. 4.6 shows that the leap becomes larger as the partial pressure of oxygen becomes higher. So, oxygen seems to cause the "late discharge" by negative ion formation.

In Fig. 4.7, the results in oxygen and in nitrogen are plotted on one plane. The vertical axis is the delay time τ_d , and the horizontal axis is the applied voltage V_k . The open circle is the result in oxygen, and the closed circle is the result in nitrogen. The transit time of electron and oxygen negative ion between electrodes are calculated by the following process and plotted on the plane as a line.

In the experiment, the discharge was triggered in the range of $20\text{kV} < V_k < 50\text{kV}$, i.e.

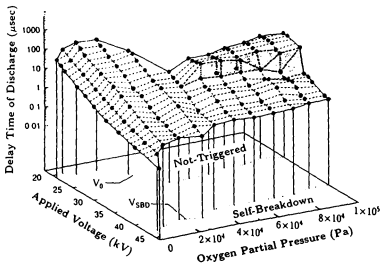


Fig. 4.5: Delay time of discharge versus applied voltage and partial pressure of oxygen.

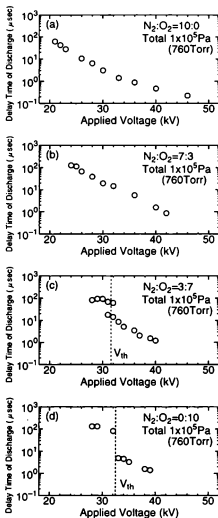


Fig. 4.6: The relation between delay time of discharge and applied voltage. $\text{N}_2:\text{O}_2 =$ (a)10:0, (b)7:3, (c)3:7, and (d)0:10.

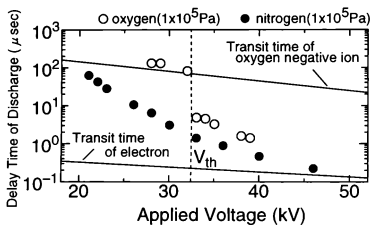


Fig. 4.7: The delay time of discharge and applied voltage in oxygen and in nitrogen. The transition time of both electron and negative ion is plotted as a line.

$9.9 \times 10^{-2} < E/p < 2.5 \times 10^{-1} \text{V}/(\text{cm} \cdot \text{Pa})$). In the low E/p , less than several tens, the drift velocities of electron and ion are in proportion to the field E . Since the mobility of the oxygen negative ion is $1.4 \times 10^3 \text{cm}^2/(\text{V} \cdot \text{sec})^{17}$, the transit time of the oxygen negative ion between electrodes is given as $\tau = d/(1.4 \times 10^3 E) = d^2/(1.4 \times 10^3 V_g)$. The transit time of the electron is calculated referring to the relation between the drift velocity of the electron and E/p which is shown in ref. 18.

The transit time of the oxygen negative ion agrees well with the delay time of "late discharge". The delay time of "early discharge" approaches the transit time of the electron as the applied voltage becomes higher. So, the oxygen negative ion seems to be dominant in the "late discharge". On the other hand, the electron avalanche seems to become dominant in the "early discharge" with the increase in the applied voltage.

4.3.3 Discussion

Since the "late discharge" seems to be caused by oxygen negative ions, the mechanism of the leap is described from the viewpoint of the generation and disappearance of them.

The photodetachment cross sections of O^- and O_2^- versus photon energy are shown in Fig. 4.8^{19,20)}. Though the cross section of O_2^- is in proportion to the photon energy, that of O^- has a threshold value of the photon energy. When the photon energy becomes higher than the threshold value, the cross section of O^- increases drastically. Since the delay time of discharge in the experiment has the leap, the electron detachment of O^- seems to occur, i.e. $\text{O}^- + e \rightarrow \text{O} + 2e$. This agrees with the fact that the seed electrons are formed by the electron detachment of O^- in the discharge which is triggered by laser irradiation between a gap¹⁴⁾.

The electron collision detachment cross section σ is obtained as follows.

$$\sigma = \frac{\langle \sigma v \rangle}{\langle v \rangle} = \int_0^\infty \sigma_{\text{photo}}(\epsilon) F(\epsilon) \sqrt{\frac{\epsilon}{\epsilon_0}} d\epsilon, \quad (4.1)$$

where $\sigma_{\text{photo}}(\epsilon)$ is the photodetachment cross section, $F(\epsilon)$ is an energy distribution function.

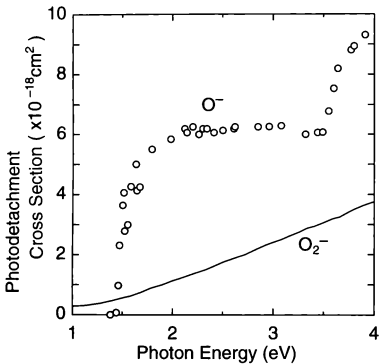


Fig. 4.8: Photodetachment cross sections of O_2^- and O^- . ^{19,20)}

and ϵ_0 is the mean electron energy given by the electric field between two successive collisions. Since this process is an electron collision, the electron energy obeys the Maxwell-Boltzmann distribution function as follows:

$$F(\epsilon) = \frac{3\sqrt{3}}{\sqrt{2\pi}\epsilon_0^{3/2}} \sqrt{\epsilon} \exp\left[-\frac{3\epsilon}{2\epsilon_0}\right]. \quad (4.2)$$

The ϵ_0 is given as follows:

$$\epsilon_0 = \lambda_e \frac{V_k}{d}, \quad (4.3)$$

where λ_e is the mean free path of the electron, V_k is the applied voltage between electrodes, and d is the gap distance. Here, by substitution of eqs.(4.2) and (4.3) into eq.(4.1), the electron collision detachment cross section is obtained as follows:

$$\sigma = \int_0^\infty \sigma_{\text{photo}}(\epsilon) \frac{3\sqrt{3}\epsilon}{\sqrt{2\pi}(\lambda_e V_k/d)^{3/2}} \exp\left[-\frac{3\epsilon}{2\lambda_e V_k/d}\right] d\epsilon. \quad (4.4)$$

The σ versus mean electron energy is obtained from this equation, and the result is shown in Fig.4.9. In the experiment, the leap of the delay time occurs in the range of $28\text{kV}(\text{N}_2 : \text{O}_2 = 6 : 4) \leq V_k \leq 32\text{kV}(\text{N}_2 : \text{O}_2 = 0 : 10)$. The value of λ_e in oxygen is $3.6 \times 10^{-5}\text{cm}^{23)}$, and that in nitrogen is $3.4 \times 10^{-5}\text{cm}^{23)}$. So, the mean free path of the electron in the mixture ($\text{N}_2:\text{O}_2=6:4$) is $3.48 \times 10^{-5}\text{cm}$. Then eq.(4.3) gives the range of ϵ_0 as $0.49\text{eV}(\text{N}_2 : \text{O}_2 = 6 : 4) \leq \epsilon_0 \leq 0.58\text{eV}(\text{N}_2 : \text{O}_2 = 0 : 10)$. The first excitation potential of nitrogen, which is 5.23eV , is much higher than the threshold energy value of detachment of O^- , which is less than 1eV (cf. Fig. 4.9), and nitrogen never forms negative ions. Then, it is sufficient to consider the detachment and attachment processes of the oxygen negative ion. As shown in Fig. 4.9, in this range the electron collision detachment cross section of O^- increases drastically. This agrees well with the experimental results. On the other hand, as shown in Fig. 4.10²²⁾, the probability of attachment for electrons in oxygen has no threshold, and it shows gentle change against E/p . The "late discharge" is caused by the decrease in mobility of negative particles and they seem to be oxygen negative ions which are formed by the electron attachment. In the "fast discharge",

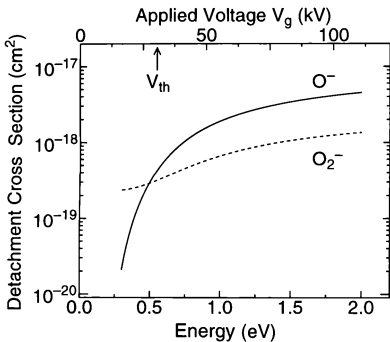


Fig. 4.9: Collision electron detachment cross sections of O^- and O_2^- .

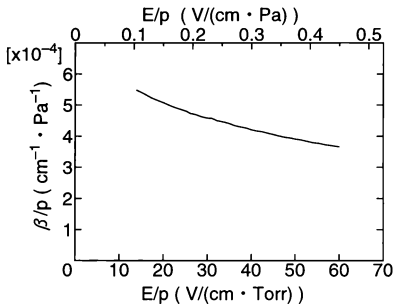


Fig. 4.10: Probability of attachment for electrons in oxygen. ⁴⁴

the negative particles are mainly electrons. Then the leap of delay time of discharge from the "late discharge" to the "fast discharge" seems to be caused by the increase in mobility of negative particles when the detachment of oxygen negative ion is over the electron attachment to oxygen.

Since oxygen atoms are unstable and rare in the air, the oxygen negative ions O^- seem to be created by the attachment of the electrons to oxygen atoms produced by the laser-produced plasma.

4.4 Summary

The correlation between the path of electrical discharge triggered by the XeCl laser-produced plasma and the discharge current is observed. When the discharge path avoids the laser-produced plasma, the current has the second peak between the first peak immediately after the laser injection and the flashover. On the other hand when the discharge path goes through the plasma, it has no peak between the first peak and the flashover. This result shows that the mechanisms of discharge are different between when the discharge path goes through the plasma and when it avoids the plasma.

The delay time of discharge versus the applied voltage between electrodes and versus oxygen partial pressure was investigated in the discharge triggered by a laser-produced plasma in the mixture of oxygen and nitrogen. It was shown that the delay time has two styles of "late discharge" and "early discharge". In the "late discharge", the delay time of discharge agrees with the transit time of an oxygen negative ion between electrodes. On the other hand, in the "early discharge", the delay time approaches the transit time of an electron between electrodes, as the applied voltage increases. As the applied voltage increases, the delay time becomes shorter, and at the threshold voltage, the delay time leaps between "late discharge" and "early discharge".

The calculation of the electron detachment cross section shows that the leap of delay time is caused by changing of negative particles between oxygen negative ion O^- and electron due to changing in the balance of electron attachment to oxygen and electron detachment of O^- .

References

- [1] J. R. Bettis and A. H. Guenthe : "Subnanosecond-Jitter Laser-Triggered Switching at Moderate Repetition Rates", *IEEE Journal of Quantum Electronics*, **QE-6**, 483-491 (1970)
- [2] T. Noguchi, M. Yano, T. Shimomura and K. Horii : "Triggering Mechanism of a Laser-Triggered Spark Gap", *Trans. I.E.E.J.*, **92-A** No.10, 449-456 (1972) [in Japanese]
- [3] N. Sato and S. Sakamoto : "Study of Laser Triggered Breakdown Mechanism in Air", *Trans. I.E.E.J.*, **95-A**, No.6, 247 (1975). [in Japanese]
- [4] Y. Kawada and T. Hosokawa : "Breakdown mechanism of a laser triggered spark gap in a uniform field gap", *J. Appl. Phys.*, **62**, 2237-2242 (1987).
- [5] Leonard M. Ball : "The laser lightning rod system: Thunderstorm domestication", *Applied Optics*, **13**, 2292-2296 (1974)
- [6] G. N. Aleksandrov, V. L. Ivanov, G. D. Kadzov, V. A. Parfenov, L. N. Pakhomov, V. Yu. Petrun'kin, V. A. Podelevskii and Yu. G. Selezev : "Effect of a laser produced ionization channel on a long discharge in air", *Soviet Physics Technique Physics*, **22**, 1233-1234 (1977)
- [7] T. Uchiyama, M. Hirohashi, H. Miyata and T. Sakai : "Study of Triggering Lightning by using TEA CO₂ Laser", *Rev. Laser Eng.*, **16**, 267-277 (1988) [in Japanese]

- [8] T.Shindo, Y.Aihara, M.Miki and T.Suzuki : "Model Experiments of Laser Triggered Lightning", *IEE Transactions on Power Delivery*, **8**, 311-317 (1993)
- [9] D. Wang, Z.-I. Kawasaki, K. Matsuura, Y. Shimada, S. Uchida, C. Yamanaka, E. Fujiwara, Y. Izawa, N. Simokura and Y. Sono : "A preliminary study on laser-triggered lightning", *Journal of Geophysical Research*, **99**, 16907-16912 (1994)
- [10] M. Jinno, M. Kubo and R. Itatani : "Triggering Discharge and Guiding Discharge Path by weak Ionized Channel with Different Wavelength Laser Beams", *Trans. I.E.E.J.*, **115-A**, 595-604 (1995) [in Japanese]
- [11] M. Kubo, M. Jinno, H. Morioka, H. Ozaki, R. Itatani, Y. Sono and T. Nagai : "The fundamental research on laser triggering of lightning IV", *I.E.E.J. Papers of HV*, **HV-91-96** (1991) [in Japanese]
- [12] M. Kubo, R. Itatani and S. Matsumura : "Basic Research for Laser Triggered Lightning - Influence of Wavelength of Laser on Atmospheric Spark Discharge -", *Trans. I.E.E.J.*, **112A**, 620-628 (1992) [in Japanese]
- [13] M. Jinno, H. Morioka, H. Ozaki, M. Kubo, R. Itatani, Y. Sono and T. Nagai : "The fundamental research on laser triggering of lightning VII", *I.E.E.J. Papers of ED*, **ED-92-72** (1992) [in Japanese]
- [14] D. Sakai, K. Hidaka and T. Kouno : "The research about a laser guided discharge", *I.E.E.J. Papers of ED*, **ED-93-55** (1993) [in Japanese]
- [15] D. Sakai, K. Hidaka and T. Kouno : "The research about a laser guided discharge (Vol. 2)", *I.E.E.J. Papers of ED*, **ED-93-175** (1993) [in Japanese]
- [16] K. Hidaka, D. Sakai and T. Kouno : "Laser Trigger Effect on Induced Electrical Discharge", *Trans. I.E.E.J.*, **115-A**, 622-629 (1995) [in Japanese]

- [17] S. Ohtori, T. Sekiguchi and T. Kouno : *Deuri-Kitai-Ron* (Ionized Gases), (I.E.E.J., Tokyo) Chap.2, p.54 (1969) [in Japanese]
- [18] Y. Hatta: *Kitai-Houden* (Discharge in Gases), (Kindai-Kagau-Sha, Tokyo) Chap.3, p.79 (1968) [in Japanese]
- [19] F. A. Boylett and B. G. Williams : *Brit. J. Appl. Phys.*, **18**, 593 (1967).
- [20] H. S. W. Massey : *Electronic and Ionic Impact Phenomena*, (Oxford, Oxford), Vol.2. (1967)
- [21] S. Takeda : *Kitai-Houden-no-Kiso* (Basics of Discharge in Gases), (Tokyo-Denki-Daigaku-Shuppan-Kyoku, Tokyo), Chap.1, p.14. (1990) [in Japanese]
- [22] S. C. Brown : *Basic Data of Plasma Physics, 1966*, (The M.I.T. Press, Massachusetts, 1967), Chap.6, p.200 (1967).

Chapter 5

Triggering Electrical Discharge and Guiding its Path by Weakly Ionized Channel with Different Wavelength of Laser Beams

5.1 Introduction

After the first report of an optical air breakdown by Maker in 1962¹⁾, in 1974 Ball proposed²⁾ the Laser Triggering of Lightning as an application of optical breakdown. After that many studies have been carried out. Now the method using a laser-produced plasma channel (called the plasma channel method)³⁻¹⁰⁾ and the method using a weakly ionized channel (called the weakly ionized method)¹¹⁾ are proposed.

As the fundamental research of the plasma channel method, the experiments of guiding a discharge path in the meter-class gap applied impulse voltage have been carried out, and the timing condition between laser oscillation and voltage application has been reported^{5,8)}. Moreover the required energy of CO₂ laser for actual Laser Triggering of Lightning is estimated^{4,10)}. Though the field experiment of Laser Triggering of Lightning has also been carried out by Kawasaki et al.^{12,13)}, they have never succeeded.

On the other hand, regarding the weakly ionized method, the author's group has already reported¹⁴⁻¹⁶⁾ that the weakly ionized part produced by laser irradiation triggers and guides a discharge and that seed electrons are produced by the photodetachment of O^- in the cm-class gap to which DC voltage is applied. Nakamura et al.¹¹⁾ estimated and reported the required intensity of KrF laser beam for actual Laser Triggering of Lightning.

The plasma channel method using a single laser beam has a fatal problem i.e. the plasma channel protects itself from expanding due to absorption and reflection of laser energy by the plasma channel itself. As a resolution of this problem the author's group proposed the Cross-Beam Method^{17,18)}.

In this chapter, the triggering and guiding of an electrical discharge effect of XeCl laser, of CO_2 laser and of simultaneous use of both of them are investigated as the fundamental research for Cross Beam Laser Triggering of Lightning. As shown in Fig. 5.1(b) (Fig. 5.2(b) is the sketch of it), the "triggered discharge" means the flashover by a laser-produced plasma between the electrodes to which the voltage below the self-breakdown threshold is applied, and it is not necessary to take notice of whether the discharge path is through the plasma or not. The "guided discharge" means the electrical discharge whose path runs along the laser light path and the length of which along the light path L_k is longer than the length of the plasma L_p along the light path, as shown in Fig. 5.1(a) and Fig. 5.2(a). Then when the "guided discharge" occurs, $L_k \geq L_p$, and when only the "triggered discharge" occurs, $L_k < L_p$.

In this chapter, the guiding effect of the weakly ionized channel produced by the XeCl laser, the triggering effect of the plasma produced by the CO_2 laser, and the effect of simultaneous use of them on the electrical discharge between the electrodes with DC voltage applied are investigated and described. Moreover, the quantity of electrons in the weakly ionized channel is measured and the required electron density for guiding a discharge path is estimated.

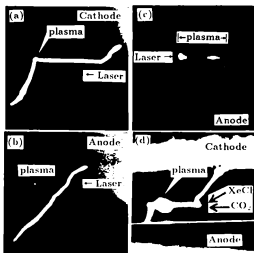
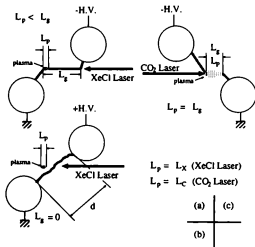


Fig. 5.1: Triggered and guided Discharge by laser. (a) Triggered and guided discharge by XeCl laser. (b) Triggered discharge by XeCl laser. (c) Triggered discharge by CO₂ laser. (d) Triggered and guided discharge by XeCl laser and CO₂ laser.



Gap distance $d=40\text{mm}$

Fig. 5.2: Sketches of Fig.5.1

5.2 Experimental Equipment

The characteristics of the XeCl laser and the CO₂ laser are shown in Table 5.1. The output energy of the laser beam was measured by the Joule meter (J50 MOLECTRON). The electrodes were brass rods with hemispherical ends. The length of the rods was 600mm. The diameter of them was 30mm. As shown in Fig. 5.3, two rods were set horizontal like uneven parallel bars and the distance between them was 40mm. The arrangement of electrodes and laser beam is shown in Fig. 5.3. The origin O is set to the point where a plasma is produced. The z -axis is set vertical, the x -axis is parallel to each electrode. The laser beam was always injected vertical to the z -axis. The line AB connects the mid point of the axis line of each electrode, and it exists on the yz plane. The electric field between electrodes becomes maximum on the line AB. The angle φ_V made by the line AB and the y -axis was always set to 40°. The angle θ made by the laser beam and the electric field was varied by changing the angle φ_H made by the laser beam and the y -axis.

In order to apply DC high voltage, a DC power supplier (DCG-100K.10L Nichicon) was used. One of the electrodes was earthed and DC high voltage was applied to the other one. By changing the earthed electrode and the polarity of the power supply, 4 combinations were examined as follows; (1)positive polarity - plasma produced near the anode, (2)positive - near the cathode, (3)negative - near the anode, and (4)negative - near the cathode. When the voltage was applied to the electrode L, the electrode U is ground side and both of the directions of the x -axis and the z -axis were inverted. In this electrodes system, a self-breakdown occurs at the ends of the electrodes if the applied voltage is over 80kV. The self-breakdown never occurs at the center of the electrodes if the applied voltage is below 90kV.

In order to measure the electrical discharge current and the delay time of the discharge, the current probe system (A6303 and AM503 Tektronics) was used. This system was set to the earthed line from the electrode. The photographs of electrical discharge were taken by the still

Table 5.1: The Characteristics of lasers used in the experiment

Characteristics	Laser	
	XeCl	CO ₂
Wavelength	308nm	10.6 μ m
Maximum Output Energy	400mJ	7J
Peak Power	13.3MW	14.5MW
FWHM of First Spike Part	25nsec	120nsec
Pulse width of Tail Part	—	2.5 μ sec

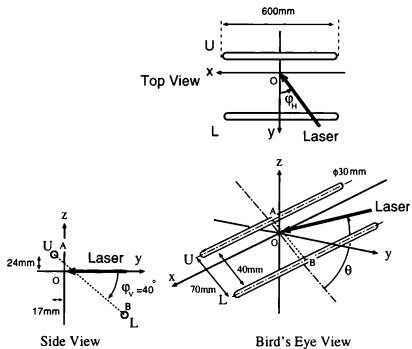


Fig. 5.3: Arrangement of electrodes and laser beam.

video camera system (MS-C110 Minolta).

The quantity of electrons on the laser light path was measured by the self-made charge collector as shown in Fig. 5.4. This charge collector was made of two electrodes and a spacer. The distance between electrodes was 10mm, the length of electrodes along the laser light path was 5mm. The capacitance was determined to $0.01\mu\text{F}$ referring to the results of examination. The applied voltage between the electrodes was set to 4.0kV so as to balance the recombination and ionization. The voltage of the capacitance was measured, then the quantity of electrons were obtained.

5.3 Triggering and Guiding an Electrical Discharge with XeCl Laser

In this section, the triggering and guiding of an electrical discharge by a XeCl laser are experimentally investigated and the quantity of electrons on its light path is measured.

5.3.1 Experimental Setup

In the system shown in Fig. 5.3, a plasma and a weakly ionized channel were produced by the XeCl laser beam which is focused by the quartz lens of 475mm focal length. The plasma position (the origin O), where both the trigger and guide effect become most effective, was found when the positive DC voltage was applied to the electrode U and the electrode L was earthed. The plasma position was consequently determined as shown in Fig. 5.3. The distance from the point A, the midpoint of the electrode U, to the z-axis was 17mm, from the point A to the y-axis was 24mm. In this alignment, the experiments were carried out for 4 combinations described in section 5.2.

The energy of the XeCl laser beam going into the lens was kept at 200-240mJ. The laser pulse was detected by the photo-tube (R1193-U05, HAMAMATSU). The discharge current was

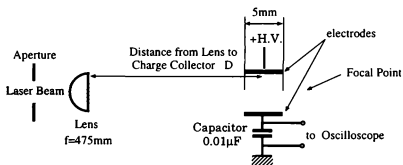


Fig. 5.4: Setup for measurement of the density of a plasma.

detected by the current probe. Then the delay time of discharge from the laser injection τ_d was measured in this system. The length of the discharge path expanding along the laser light path (L_R) and that of the laser-produced plasma (L_x) were measured from the still-photographs. In this system, V_{50} (the 50% flashover voltage), L_R , and τ_d versus the laser incident angle θ were measured. Moreover, the dependence of L_R and τ_d on the applied voltage between electrodes V_g was observed.

As shown in Fig. 5.4, the current induced by the charges, which are produced between electrodes by the XeCl laser beam, was integrated by the capacitance. An aperture was set on the XeCl laser light path in order to prevent the laser beam from irradiating the electrodes. The charging voltage wave of capacitance consists of the rapid changing part (Phase1) and the gentle rising part (Phase2). The charge $Q(= CV)$ accumulated in the capacitance is calculated from the charging voltage of capacitance V when the voltage wave of Phase2 becomes constant^{11,19)}. The quantity of charge was measured when the XeCl laser energy was 4.6mJ and 195mJ. A plasma is never produced at 4.6mJ because it is too low. The threshold value of the XeCl laser energy is about 50mJ. At 195mJ of energy, a plasma is produced and the energy is sufficiently over the threshold of plasma formation. The charge distribution was measured by changing the distance between the lens and the charge collector.

5.3.2 Experimental Results

In Fig.5.1, the examples of the "guided discharge" (a) and the "triggered discharge" (b) by the XeCl laser beam are shown. When the photograph (a) was taken, the applied voltage between electrodes was 80kV of negative polarity. The left hand electrode was earthed. The negative voltage was applied to the right hand electrode. The laser beam was injected from the right side, and a plasma was produced near the anode. When the photograph (b) was taken, the alignment was the same as the photograph (a). The positive voltage of 65kV was applied to

the right hand electrode, and a plasma was produced near the cathode.

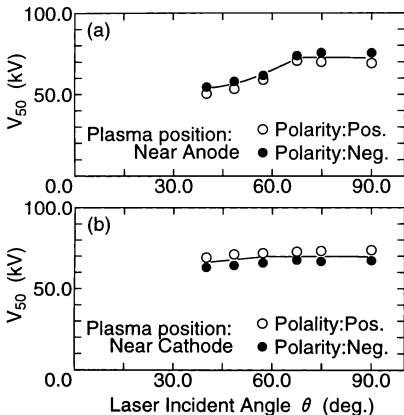
In Fig. 5.5, the 50% flashover voltage V_{50} versus the laser incident angle θ is shown. The results when the plasma was produced near the anode are (a), and those near the cathode are (B). When θ is larger than 60° , V_{50} has no dependence on θ . When a plasma is produced near the anode, at $\theta < 60^\circ$ V_{50} is lower than when a plasma is produced near the cathode. Thus V_{50} is determined by the plasma position, not by the polarity of the applied voltage between the electrodes.

The length of guided discharge path L_g and the delay time of discharge τ_d versus the laser incident angle θ at $V_g=80\text{kV}$ are shown in Fig. 5.6. The L_x is the length along the laser light path of the plasma produced by the XeCl laser. These results show that both the guided length L_g and the delay time τ_d have no dependence on the polarity of the applied voltage. At $\theta < 75^\circ$, the guided length L_g has no dependence on plasma position. At $\theta > 75^\circ$, the discharge path does not go through the plasma ($L_g < L_x$) when the plasma is produced near the cathode. On the other hand, it goes through the plasma ($L_g > L_x$) when the plasma is produced near the anode. The delay time τ_d becomes constant when the plasma is produced near the anode at $\theta > 70^\circ$ or near the cathode at $\theta > 60^\circ$. The polarity of the applied voltage has no effect on the guided length L_g and the delay time τ_d . However they are determined by the laser incident angle θ and plasma position the same as the results of V_{50} .

In Fig. 5.7, the guided length L_g versus $\cos\theta/\sin\theta$ at $V_g=80\text{kV}$ is shown. This result gives an experimental formula between θ and L_g as follows.

$$L_g = 17.2 \times \frac{\cos\theta}{\sin\theta} \quad (\text{mm}) \quad (5.1)$$

The guided length L_g and the delay time τ_d versus the applied voltage V_g are shown in Fig. 5.8. When the plasma was produced near the anode, the mean values of them are plotted as a dotted circle and a dotted triangle. All the results are plotted as an open circle and an open triangle when the plasma was produced near the cathode, because the number of trials

Fig. 5.5: Relation between θ and V_{50} .

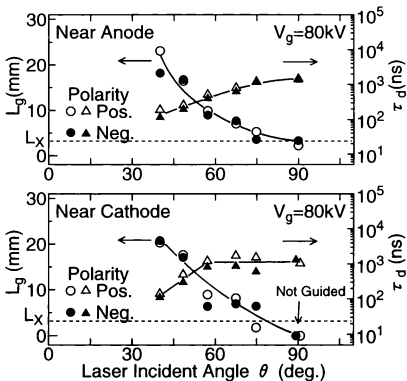


Fig. 5.6: Guided length of discharge path L_g and delay time of discharge τ_d versus laser incident angle θ .

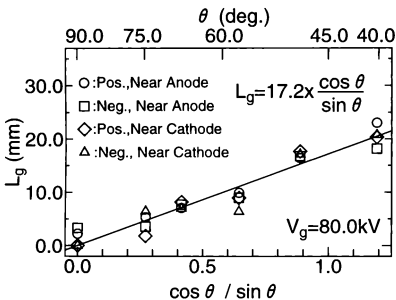


Fig. 5.7: Guided length of discharge path L_g versus laser incident angle θ .

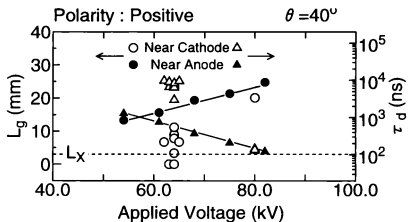


Fig. 5.8: Guided length L_g and delay time of discharge τ_d versus applied voltage V_k .

is insufficient to average. When the plasma position is near the anode, the guided length L_g and the delay time τ_d change continuously obeying the change of the applied voltage V_g . At $V_g=80\text{kV}$, they have no dependence on the plasma position. However, at $V_g=60\text{kV}$, when the plasma position is near the anode, the guided length L_g becomes longer and the delay time τ_d becomes shorter than those of near the cathode. Moreover, at $V_g=60\text{kV}$, when a plasma is produced near the cathode, the discharge style seems to be the "late discharge" which is described in Chapter 4.

The charge distribution on the laser light path is shown in Fig. 5.9(a) and (b). Figure 5.9(a) is the result when the energy of the XeCl laser was 195mJ, and (b) shows all the results using the XeCl laser or the CO₂ laser. The experiments and results using a CO₂ laser are described in section 5.4. When the plasma is produced, the quantity of charge is more by 3 orders of magnitude than that without plasma formation. In both cases, there is no charge and weak ionization at the point where the distance from the focal point is more than 25mm.

5.3.3 Discussion

As shown in Figs. 5.5, 5.6, and 5.8, the 50% flashover voltage V_{50} , the delay time of discharge τ_d and the guided length of discharge path L_g all depend on the plasma position. Moreover when the plasma position is near the anode, the delay time τ_d becomes shorter and the guided length L_g becomes longer than when it is near the cathode. These results show that a discharge is triggered and guided effectively when a plasma is produced near the anode. Since the effect of ground, i.e. the polarity effect, is little in this electrodes system, the polarity of applied voltage between the electrodes has no effect.

The jump of delay time of discharge is not observed when the plasma position is near the anode as shown in Fig. 5.8. However, the author's group has already reported²⁰⁾ that the jump of delay time of discharge occurs whenever the plasma position is near the anode or near the

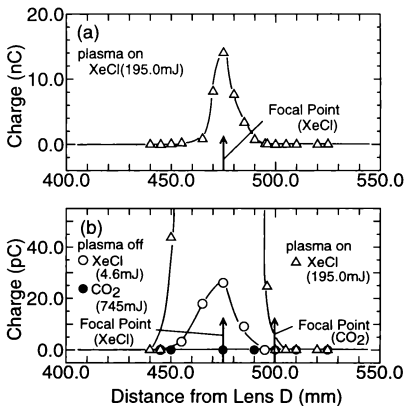


Fig. 5.9: Detected charge on the laser light path.

cathode. So the reason why the jump does not occur seems to be that the applied voltage, where the jump should occur, may be lower than the minimum applied voltage for triggering an electrical discharge. The guided length of discharge path becomes shorter as the delay time of discharge becomes longer. Then an electrical discharge is triggered and guided effectively when a plasma is produced near the anode because the jump of delay time of discharge may occur at lower applied voltage when the plasma position is near the anode than when it is near the cathode.

As shown in Fig. 5.1, when an electrical discharge is triggered by a XeCl laser, the discharge path expands over the length of the laser-produced plasma. Moreover, as shown in Fig. 5.9, electrical charge exists on the XeCl laser light path near the focal point. Then a XeCl laser beam produces the weakly ionized channel on its light path, and the weakly ionized channel seems to work effectively in guiding of the discharge path.

Since a laser-produced plasma has the effect of triggering an electrical discharge^(21,22), and since the weakly ionized channel has the effect of guiding an electrical discharge path, the characteristic of the guided length of discharge path L_g versus the applied voltage between electrodes V_g is accounted from the results shown in Figs. 5.5, 5.6, and 5.8 according to the laser incident angle θ as follows :

- 1) At the small laser incident angle ($\theta < 50^\circ$) — Since the component of the electric field vector along the laser light path is large, as the applied voltage increases, the guided length of discharge path becomes longer by the guiding effect of the weakly ionized channel.
- 2) As the angle increases ($50^\circ < \theta < 70^\circ$), the component of the electric field vector along the laser light path becomes small. Then the guiding effect of the weakly ionized channel becomes small, consequently the effect of applied voltage between electrodes on the guided length of the discharge path becomes small.

- 3) As the angle increases more ($70^\circ < \theta$), the guiding effect of the weakly ionized channel is lost because the component of the electric field vector along the laser light path becomes almost zero. Then only the trigger effect of the laser-produced plasma remains. So the 50% flashover voltage and the delay time of discharge become constant, the guided length of discharge path becomes shorter than the plasma length, and the discharge path sometimes avoids the plasma.

The vector of electric field E applied between electrodes is split into two components; the one along the laser light path $E_{\parallel} = E \cos \theta$ and the other vertical to it $E_{\perp} = E \sin \theta$. The E_{\parallel} accelerates the electric charge along the laser light path. On the other hand, the E_{\perp} sweeps out the electric charge from the weakly ionized channel. So, suppose that the guided length of discharge path L_g is in proportion to E_{\parallel} and is in inverse proportion to the increasing function $f(E_{\perp})$ of E_{\perp} . Then the formula (5.1) is obtained by the expansion of $f(E_{\perp})$ into power series and the neglect of the terms higher than the second order. Therefore this supposition seems to be proper.

As shown in Fig. 5.8, the leap of delay time of discharge occurs when the plasma position is near the cathode. The intensity of the electric field at the plasma position is calculated considering the electrodes as infinite parallel cylindrical conductors. Since the intensity of the electric field is 16.7kV/cm when the applied voltage V_g is 80kV, the drift velocity of electrons is obtained as 9.0×10^6 cm/sec²³⁾. So the transit time of electrons between the electrodes is obtained as 4.4×10^2 nsec. On the other hand the drift velocity of negative ions is obtained as 2.1×10^4 cm/sec since the intensity of the electric field is 13.6kV/cm at $V_g = 65$ kV²⁴⁾. Then the transit time of negative ions is obtained as 1.9×10^2 μsec. As shown in Chapter 4, the leap of delay time discharge is caused by the changing of negative particles between electrons and oxygen negative ions O^- according to the intensity of the electric field. The transit time of electrons at $V_g = 80$ kV agrees with the delay time of discharge. However, that of negative ions

at $V_g = 65\text{kV}$ is different from the delay time of discharge. i.e. the delay time of discharge is smaller by one order of magnitude than the transit time. When a discharge is triggered and guided by a laser-produced plasma and a weakly ionized channel, the mechanism of discharge seems to be different from the discharge triggered by only a laser-produced plasma. So, the weakly ionized channel may causes the difference.

5.4 Triggering and Guiding an Electrical Discharge with CO₂ Laser

In this section, the triggering and guiding of an electrical discharge by a CO₂ laser, which is oscillated with high efficiency and transmitted in air with low loss, is experimentally investigated and the quantity of electrons on its light path is measured.

5.4.1 Experimental Setup

The energy of the CO₂ laser beam which goes into the lens was set to 3.5-4.4J. The plasma position was set near the anode considering the results of experiments using a XeCl laser as described in section 5.3. In the system shown in Fig. 5.3, the CO₂ laser beam was focused by the KCl lens of 130mm focal length when the laser incident angle $\theta = 40^\circ$, or was focused by the ZnSe lens of 500mm focal length at $\theta = 90^\circ$. The electrical discharge was triggered by the plasma produced by the CO₂ laser beam and the trigger and the guide effects were observed. In addition, at $\theta = 40^\circ$, the 50% flashover voltage V_{50} was measured.

The quantity of electric charges on the CO₂ laser light path was measured in the same way as the case using a XeCl laser. The energy of the CO₂ laser which goes through the lens was set to 745mJ, which is slightly below the threshold value of plasma formation 750mJ, so as not to produce a plasma.

5.4.2 Experimental Results and Discussion

Both the voltage where the flashover probability becomes 1.0 and the minimum voltage for triggering an electrical discharge have no dependence on the laser incident angle. So the 50% flashover voltage seems also to have no dependence on the laser incident angle.

The photograph of the electrical discharge triggered by the plasma produced by the CO₂ laser is shown in Fig. 5.1(c). When this photograph was taken, 80kV of negative voltage was applied on the left hand electrode, the right hand one was earthed, and the laser beam was injected from the left side at $\theta = 40^\circ$. Since the bright part of the discharge path along the laser light path is the laser-produced plasma, the discharge path is never guided over the plasma length when a CO₂ laser is used.

Since a CO₂ laser never produces any weakly ionized channel on its light path as shown in Fig. 5.9(b), both the trigger effect and the guide effect never seem to be influenced by the laser incident angle.

The 50% flashover voltage is shown in Table 5.2. It was measured when the electrical discharge was triggered by the plasma produced by the CO₂ laser and the laser incident angle was 40°. When the CO₂ laser is used, the V_{50} is 20kV lower than that when the XeCl laser is used. Thus the plasma produced by the CO₂ laser is more effective for triggering an electrical discharge than that produced by the XeCl laser. The volume size of the plasma produced by CO₂ laser is about 800 times as large as that produced by XeCl laser as shown in Chapter 2. This difference in plasma size seems to cause the difference in trigger effect between the CO₂ laser and the XeCl laser.

Table 5.2: Variation of V_{50} by laser wavelength (plasma position is near the anode).

50% flashover voltage	laser			
	XeCl	CO ₂	XeCl + CO ₂	CO ₂
Positive voltage (kV)	54.65	not triggered	36.30	32.61
Negative voltage (kV)	50.55	not triggered	36.10	32.45
focal length of the lens(mm)	500	500	500(XeCl) 500(CO ₂)	130
laser incident angle θ (deg.)	40	40	40(XeCl) 90(CO ₂)	40
plasma formation	formed	not formed	formed	formed

5.5 Triggering and Guiding an Electrical Discharge with XeCl laser and CO₂ Laser

In this section, the triggering and guiding of an electrical discharge using a XeCl laser and a CO₂ laser simultaneously is experimentally investigated in order to estimate the effect of combination of different wavelengths of laser beams.

5.5.1 Experimental Setup

The XeCl laser beam was injected along the y -axis and was focused near the anode by the quartz lens of 475mm focal length. The CO₂ laser beam was injected along the x -axis at $\theta = 90^\circ$ and was focused on the focal point of the XeCl laser beam by the ZnSe lens of 500mm focal length. Already the author's group reported²⁵⁾ that there is no difference in the trigger effect between the plasma produced by superposition of a XeCl laser and a CO₂ laser, each energy of which has energy below the threshold value of plasma formation, and the plasma which is produced primarily by a XeCl laser and is heated up by a CO₂ laser. Then, in this experiment, the plasma was produced by the XeCl laser with 200-240mJ of energy, and it was heated and enlarged in volume by the CO₂ laser with 3.5-4.4J of energy. The CO₂ laser was injected 140nsec later than the injection of the XeCl laser in order to heat and enlarge the primary plasma produced by the XeCl laser. In this system, the delay time of electrical discharge and the guided length of discharge path versus the applied voltage between electrodes were observed. Moreover, the 50% flashover voltage was measured.

5.5.2 Experimental Results

The photograph of the electrical discharge triggered by the XeCl laser and the CO₂ laser is shown in Fig. 5.1(d). The 80kV of negative DC voltage was applied to the upper electrode and

the lower electrode was earthed. The XeCl laser beam was injected from the far side to the near side of the photograph, and the CO₂ laser was injected from the right side. The plasma was produced near the anode. As shown in this photograph, an electrical discharge can be triggered and guided by the superposition of a XeCl laser and a CO₂ laser.

The 50% flashover voltage is shown in Table 5.2. Though the CO₂ laser can not trigger an electrical discharge when it is focused by the ZnSe lens of 500mm focal length, the triggering and guiding of an electrical discharge is achieved by superposition of the XeCl laser and the CO₂ laser. By the superposition, the volume size of the plasma is enlarged and the V_{50} is reduced compared with those using only a XeCl laser.

The delay time of the discharge τ_d and the guided length of the discharge path L_g versus the applied voltage V_g between the electrodes are shown in Fig. 5.10. The L_C is the length of the plasma produced by the CO₂ laser along the XeCl laser light path, and the L_X is that produced by the XeCl laser. This figure shows that a discharge is triggered at the voltage below 40kV when the CO₂ laser is superposed on the XeCl laser, though the minimum voltage of triggering an electrical discharge is about 50kV when only the XeCl laser is used. At the applied voltage $V_g \approx 40kV$, the discharge path is guided when the delay time is short, i.e. the "early discharge". On the other hand, the discharge path is not guided when the delay time is long, i.e. the "late discharge". Thus, there is a close correlation between the delay time of discharge and the guided length of the discharge path. Since there is no difference in the guided length of the discharge path between the case of using only the XeCl laser and that of using the XeCl laser and the CO₂ laser in the range of voltage ($V_g > 50kV$) where an electrical discharge is triggered by the XeCl laser, the weakly ionized channel produced by the XeCl laser seems to play a large part in guiding the discharge path. On the other hand, since an electrical discharge is triggered by the superposition of the XeCl laser and the CO₂ laser in the range of the voltage ($V_g < 50kV$) where no discharge is triggered by only the XeCl laser,

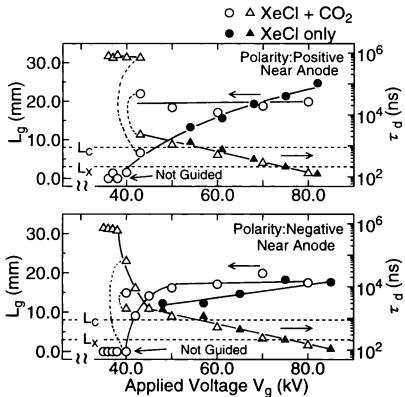


Fig. 5.10: Guided length of discharge path L_g and delay time of discharge τ_d versus applied voltage V_g using XeCl laser and CO₂ laser.

the superposition of different wavelengths of laser beams seems to be effective for triggering an electrical discharge.

5.5.3 Discussion

As shown in Fig. 5.9, the charge distribution of the XeCl laser on its light path becomes maximum at the focal points of the lens, and it decreases as the distance from the focal point increases. So, the electron density at the point, where the discharge path parts away from the laser light path, seems to be the threshold value of electron density for guiding a discharge path. As shown in Fig. 5.8, at $\theta = 40^\circ$ the maximum guided length of the discharge path is 25mm when only the XeCl laser is used. At that point, where the distance from the focal point is 25mm, the quantity of the charge, is 43.7pC when the XeCl laser energy is 195mJ as shown in Fig. 5.9. So the electron density at that point is obtained as $1.1 \times 10^{13} \text{cm}^{-3}$ because the volume size of the laser beam which goes through the charge collector is $2.51 \times 10^{-8} \text{m}^3$. On the other hand, since the quantity of electric charge at the focal point is 14000pC and since the volume size of the laser beam is $1.92 \times 10^{19} \text{m}^{-3}$, the electron density required for triggering an electrical discharge is obtained as $1.9 \times 10^{16} \text{cm}^{-3}$. This is 2000 times as high as the density of the weakly ionized channel required for guiding an electrical discharge path. These results show that in order to trigger a discharge at a voltage much lower than the self breakdown voltage, the laser-produced plasma is required, however, in order to guide a discharge path triggered by a laser-produced plasma, a plasma channel is unnecessary and a weakly ionized channel is sufficient for this role.

From the discussion about the dependence of the delay time of discharge on the applied voltage between electrodes using only a XeCl laser and regarding the guide effect of the weakly ionized channel, the correlation between the delay time and the guided length of discharge path shown in Fig. 5.10 is qualitatively accounted as follows: When a discharge path is guided by

the weakly ionized channel, the channel works effectively as a conductor, and the electric fields at both ends of the channel are increased. Then the electron avalanche is formed there and the weakly ionized channel turns into the discharge path. So, the length of discharge path which should be formed newly becomes shorter, then the delay time, i.e. the time for discharge path formation, becomes shorter. On the other hand, when a discharge path is not guided by the weakly ionized channel, the channel has no influence on the electrical discharge. In this case, the discharge path should be fully formed independently of the channel, so the delay time of discharge becomes longer. Whether the weakly ionized channel works effectively in guiding a discharge path or not is determined by the applied voltage between electrodes. When the applied voltage is high, a discharge path is guided and the delay time of the discharge becomes short. At lower voltages, the channel loses the guide effect, and the discharge path is not guided and the delay time becomes long.

Since the laser-produced plasma is effective for triggering a discharge and since the weakly ionized channel is effective for guiding a discharge path, the combination of the plasma and the weakly ionized channel is expected to be effective for the laser triggering of lightning. Here, the Hybrid Cross-Beam Laser Triggering of Lightning is proposed as shown in Fig. 5.11. By using UV lasers and IR lasers (or microwave), this method will work well not only for triggering and guiding a lightning discharge but also for plasma formation because the UV laser effectively produces seed electrons and the IR laser (or the microwave) effectively heats them up and leads them to a plasma as shown in Chapter 2. Since there is a report¹¹⁾ that the absorption of a KrF laser by the air will be 2% when it produces a 200m length of weakly ionized channel, in actual use for laser triggering of lightning, the absorption of a UV laser beam by the air is negligible.

Since the Cross-Beam method produces plasmas only at the crossing points of laser beams, too much absorption of laser energy by plasmas themselves is never caused. So this method is

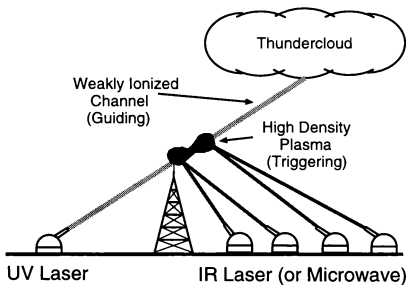


Fig. 5.11: Hybrid-Cross-Beam Laser Triggering of Lightning.

expected to achieve the effective energy transmission and plasma formation. Since the plasma should be produced near the anode for effective triggering of an electrical discharge as described in section 5.3, in the actual laser triggering of lightning the plasma position should be changed according to the polarity of the thundercloud. The Cross-Beam method has the advantage on this point, because it is easy to change the plasma position by changing the crossing point of laser beams.

5.6 Summary

The characteristics of the electrical discharge triggered by the laser-produced plasma depend on the plasma position. The plasma produced near the anode is much more effective for triggering and guiding an electrical discharge than that produced near the cathode.

The delay time of discharge versus the applied voltage leaps at a certain voltage. This leap is caused by the changing of negative charge between an electron and an oxygen negative ion as shown in Chapter 4. When the discharge path is guided, the discharge is "early discharge", otherwise, when it is not guided, the discharge is "late discharge".

The XeCl laser produces a weakly ionized channel, but the CO₂ laser never produces it. By the combination of the heating effect of the CO₂ laser and the weakly ionized channel produced by the XeCl laser, both the minimum voltage for triggering an electrical discharge and the minimum voltage for guiding a discharge path are reduced.

Though the plasma is indispensable to trigger an electrical discharge, a weakly ionized channel works sufficiently for guiding the triggered discharge by the laser-produced plasma. The required electron density for only guiding a discharge path is 1/2000 of that of the plasma for triggering an electrical discharge. The combination of different wavelengths of laser beams, such as UV and IR, will achieve the effective plasma formation, triggering an electrical discharge and guiding a discharge path. This will be useful for the Laser Triggering of Lightning.

References

- [1] P. D. Maker, R. W. Terhune and C. M. Savage : "Optical Harmonic Generation", *Quantum Electronics 2*, Columbia Univ. Press, 1559-1576 (1964)
- [2] Leonard M. Ball. : "The laser lightning rod system: Thunderstorm domestication", *Applied Optics*, **13**, 2292-2296 (1974)
- [3] T. Uchiyama, M. Hirohashi, H. Miyata and T. Sakai : "Study of Triggering Lightning by using TEA CO₂ Laser", *Rev. Laser Eng.*, **16**, 267-277 (1988) [in Japanese]
- [4] T. Shindo, Y. Aihara, M. Miki and J. Wada : "Theoretical study of laser-triggered lightning (Pt. 1) - Calculation of plasma production by a laser -", *CRIEPI Report. No.T91057* (1992) [in Japanese]
- [5] T. Shindo, Y. Aihara, M. Miki and T. Suzuki : "Model Experiments of Laser Triggered Lightning", *IEEE Transactions on Power Delivery*, **8**, 311-317 (1993)
- [6] M. Miki, Y. Aihara and T. Shindo : "Development of long gap discharges guided by a pulsed CO₂ laser", *J. Phys. D:Appl. Phys.*, **26**, 1244-1252 (1993)
- [7] T. Shindo, M. Miki, J. Wada and Y. Aihara : "Simulation of Plasma Production with Laser Propagation", *Trans. I.E.E.J.*, **115-A**, 589-594 (1995) [in Japanese]

- [8] C. Honda, T. Takuma, K. Muraoka, M. Akazaki, F. Kinoshita and O. Katahira : "Characteristics of Discharge Induced by Laser-Generated Plasmas", *Trans. I.E.E.J.*, **113-B**, 994-1002 (1993) [in Japanese]
- [9] T. Ikegami, T. Kakiuchi, K. Ebihara and M. Akazaki : "Characteristics of Electrical Discharge Induced by Excimer Laser", *Trans. I.E.E.J.*, **114-A**, 31-39 (1994) [in Japanese]
- [10] T. Uchiyama : "Laser Triggering Lightning", *Jpn. J. Plasma and Fusion*, **70**, 168-172 (1994) [in Japanese]
- [11] K. Nakamura, T. Suzuki, C. Yamabe and K. Horii : "Fundamental Research for Lightning Trigger Experiment by Using UV Lasers", *Trans. I.E.E.J.*, **113-B**, 1265-1273 (1993) [in Japanese]
- [12] Y. Ishikubo, H. Shimokura, Z. Kawasaki, K. Matsuura, N. Uchida, Y. Shimada, H. Yasuda and C. Yamanaka : "The field experiments of laser triggered lightning using CO₂ laser", *I.E.E.J. Papers of ED and HV*, **ED-94-39**, **HV-94-43** (1994) [in Japanese]
- [13] S. Uchida, Y. Shimada, H. Yasuda, K. Tsubakimoto, S. Motokoshi, C. Yamanaka, T. Yamanaka, H. Fujita, K. Matsuura, Z. Kawasaki, T. Ushio, T. Watanabe, W. Daohong, M. Adachi and Y. Ishikubo : "The field experiments of laser triggered lightning", *Rev. Laser Eng.*, **24**, 547-555 (1996) [in Japanese]
- [14] M. Kubo, A. Sumita and R. Itatani : "The triggering a spark discharge by laser irradiation and the possibility of laser triggering of lightning", *I.E.E.J. Papers of HV*, **HV-83-43** (1983) [in Japanese]
- [15] M. Kubo, A. Sumita, H. Ozaki and R. Itatani : "The triggering a DC spark discharge by UV, Visible and IR laser irradiation", *I.E.E.J. Papers of ED*, **ED-84-57** (1984) [in Japanese]

- [16] M. Kubo, R. Itatani and S. Matsumura : "Basic Research for Laser Triggered Lightning Influence of Wavelength of Laser on Atmospheric Spark Discharge -". *Trans. I.E.E.J.*, **112A**, 620-628 (1992) [in Japanese]
- [17] M. Kubo, K. Okayama, A. Taketani, N. Kosugi and R. Itatani : "The effect of simultaneous irradiation of laser beams on triggering discharge". *1989 National Convention Records of I.E.E.J.*, No.111 (1989) [in Japanese]
- [18] M. Jinno, M. Kubo, and R. Itatani : "Triggering Discharge and Guiding Discharge Path by Weak Ionized Channel with Different Wavelength Laser Beams". *The Transactions of The Institute of Electrical Engineers of Japan*, **115A**, 595-604 (1995) [in Japanese]
- [19] J. Sasaki, S. Kubodera, R. Ozaki and T. Uchiyama : "Characteristics of interelectrode flashover in air with the existence of weakly ionized plasma channel induced by a KrF laser". *J. Appl. Phys.*, **60**, 3845-3849 (1986)
- [20] G. Nagano, M. Jinno, H. morioka, M. Kubo, R. Itatani, Y. Sono and T. Nagai : "The fundamental research on laser triggering of lightning X", *I.E.E.J. Papers of ED*, **ED-93-58** (1993) [in Japanese]
- [21] M. Kubo, K. Okayama, A. Taketani, M. Jinno and R. Itatani : "The triggering a flashover by superposition of two laser beams", *I.E.E.J. Papers of ED*, **ED-89-122** (1989) [in Japanese]
- [22] M. Kubo, A. Taketani, M. Jinno, H. morioka, R. Itatani, Y. Sono and T. Nagai : "The fundamental research on laser triggering of lightning - The plasma formation and the triggering and guiding a discharge by superposition of different wavelength laser beams". *1991 National Convention Records of I.E.E.J.*, No.180 (1991) [in Japanese]

- [23] Y. Hatta : "Kitai-Houden (Electrical Gas Discharge)", Kindai-kagaku-sha, pp.79 (1960)
[in Japanese]
- [24] S. Ohtori, T. Sekiguchi and T. Kouno : "Denri-Kitai-Ron (Ionized Gas Physics)", Denki-Gakkai (I.E.E.J.), pp.54 (1969) [in Japanese]
- [25] M. Kubo, A. Taketani, M. Jinno, H. Morioka, R. Itatani, Y. Sonoji and T. Nagai : "The fundamental research on the laser triggering of lightning by superposition of laser beams". *I.E.E.J. Papers of HV*, **HV-91-2** (1991) [in Japanese]

Chapter 6

Conclusion

In this thesis plasma formation by superposition of laser beams and triggering and guiding of an electrical discharge by a laser-produced plasma and a weakly ionized channel are experimentally investigated in order to establish fundamentally the Cross-Beam Laser Triggering of Lightning. The conclusions and remaining future works are summarized in this chapter.

In Chapter 2, plasma formation by the superposition of laser beams was investigated. It becomes clear that an optical breakdown is made by superposing two laser beams, the energy of which are both limited below the threshold value of a breakdown so as not to produce a breakdown by focusing only one beam. The addition law of energy for plasma formation by superposition of laser beams of the same wavelength holds with consideration of timing, positioning, and volume size of cross focusing of laser pulses. The superposition of a CO_2 laser beam and a XeCl laser beam with fine tuning of timing and positioning reduces drastically the required energy of the CO_2 laser for plasma formation keeping the volume size of the plasma almost the same as that made by only a CO_2 laser. Thus, the combination of a CO_2 laser and a XeCl laser is effective for plasma formation because a XeCl laser produces seed electrons by its high photon energy and a CO_2 laser heats them up and leads them to a plasma by its high field and high energy.

Chapter 3 describes the experiment of plasma formation and heating in the open air by

superposition of a microwave and a XeCl laser beam. It is shown that a plasma is produced by superposition of a XeCl laser beam and a microwave. Moreover it is shown that the continuous microwave heats a plasma produced by superposition, makes it steady-state, and enlarges its volume size. By superposing a microwave on a XeCl laser, the threshold value of the XeCl laser energy for plasma formation is reduced to 20%. On the other hand, by superposing a XeCl laser beam on a microwave, the required power of microwave for plasma formation is reduced to 8%. Thus, superposition of a XeCl laser and a microwave works effectively for plasma formation and heating. A microwave of centimeter class or millimeter class is especially suitable for acceleration of seed electrons by its field. On the other hand, the IR laser and the sub-millimeter class microwave are suitable for plasma heating by their field.

In Chapter 4, the correlation between the path of electrical discharge triggered by the XeCl laser-produced plasma and the discharge current was observed in the open air. When the discharge path avoids the laser-produced plasma, the current has the second peak between the first peak immediately after the laser injection and the flashover. On the other hand when the discharge path goes through the plasma, it has no peak between the first peak and the flashover. This result shows that the mechanisms of discharge are different between when the discharge path goes through the plasma and when it avoids the plasma. Moreover, the delay time of discharge triggered by the XeCl laser-produced plasma was investigated in the mixture of oxygen and nitrogen. When oxygen exists in the mixture, the delay time has two styles of "late discharge" and "early discharge". The delay time of "late discharge" agrees with the transit time of oxygen negative ion between electrodes. The delay time of "early discharge" approaches the transit time of an electron between electrodes as the applied voltage between electrodes increases. There is the threshold voltage, where the delay time leaps between "late discharge" and "early discharge". The result of calculation of the electron detachment cross section shows that the leap of the delay time is caused by changing of negative particles triggering an electrical

discharge from oxygen negative ions O^- to electrons due to the increase in electron detachment as the applied voltage becomes higher.

In Chapter 5, the experiment on triggering and guiding an electrical discharge by a weakly ionized channel produced by a XeCl laser were carried out, and it was shown that a XeCl laser produces a weakly ionized channel on its light path and that the CO_2 laser never produces it. This weakly ionized channel guides a discharge path and in order to guide only a path of discharge triggered by a plasma, electron density is required to be higher than $1.1 \times 10^{16} m^{-3}$. This is only about 0.05% of the density required for triggering of a discharge by an air breakdown plasma. By using both the weakly ionized channel produced by a XeCl laser and the air breakdown plasma heated by a CO_2 laser, the flashover voltage is reduced and the guided length of the discharge path becomes longer than those using only a XeCl laser. Combining the air breakdown plasma and the weakly ionized channel using different wavelength laser beams, for example UV laser and IR laser, works effectively for plasma formation, and is expected to be useful for triggering of lightning and guiding a lightning path.

In conclusion, the fundamental key-problems of Cross-Beam Laser Triggering of Lightning have been clarified. They are the plasma formation by superposition of laser beams and the triggering and guiding of an electrical discharge by a laser-produced plasma and a weakly ionized channel. Moreover, the effectiveness of the Cross-Beam method on plasma formation and on triggering and guiding an electrical discharge is shown. By considering the results obtained through this work, the Hybrid-Cross-Beam method is proposed. In recent years, some research groups have adopted our Hybrid method and started fundamental studies of it. This is our great honour and pleasure as engineering scientists. In the next step, the Hybrid method should be examined in a long gap. We expect that the Hybrid-Cross-Beam method contributes to the development of practical Laser Triggering of Lightning.

Masafumi Jinno was born in Kyoto-city, Kyoto prefecture in 1966. He graduated Kyoto University in 1990, and took a Master's Degree of Engineering of Kyoto University in 1992. From 1995, he has been working at the Department of Electrical and Electronic Engineering of Ehime University. While he was in Kyoto University, he worked with the Laser and Light Source research group, and studied Laser Triggering of Lightning, plasma formation by superposition of laser beams and by superposition of microwave and laser, and laser triggered discharge. After moving to Ehime University, he continued previous work and started the study of development and measurement of light sources. He also began the study of development of immediate ignitable HID lamp and will start a study of gas insulation without Freon Gases. He is a member of the Institute of Electrical Engineers of Japan, the Japan Society of Applied Physics, and the Illuminating Engineering Institute of Japan.